THE EFFECTS OF GEOMAGNETICALLY-INDUCED CURRENTS (GIC'S) ON POWER TRANSFORMERS

(Quantitative Evaluation)

A Thesis

Presented to

The Department of Electrical Engineering

Faculty of Graduate Studies

The University of Manitoba

In partial fulfillment

of the requirements for the degree of

Master of Science

By

Saeed Arabi

September 1981

THE EFFECTS OF
GEOMAGNETICALLY-INDUCED CURRENTS (GIC'S)
ON POWER TRANSFORMERS
(Quantitative Evaluation)

BY

SAEED ARABI

A thesis submitted to the Faculty of Graduate Studies of
the University of Manitoba in partial fulfillment of the requirements
of the degree of

MASTER OF SCIENCE

ABSTRACT

Large transient fluctuations in the earth's magnetic field, triggered by solar flares, can induce voltages in the earth's surface. These induced voltages, with fundamental periods of the order of several minutes, can produce quasi-dc currents in electric power systems, termed "Geomagnetically-Induced Currents (GIC's). GIC's passing through the grounded neutral leads of power transformers, produce simultaneous ac-dc excitations resulting in half-cycle saturation of the transformers. This effect of GIC on power transformers is studied in this thesis. The produced harmonics (including fundamental), voltage drop at the secondary terminals, increased copper losses, iron losses, increased VAR demands, apparent power and the components of the apparent power are calculated as functions of GIC. The results are plotted for different core saturation characteristics. These results (graphs) may be used as well in determining several other disturbances in power systems caused by GIC.

ACKNOWLEDGEMENTS

I wish to express my sincere gratitude to Professor M.Z. Tarnawecky, my advisor, for his guidance.

Appreciation is also expressed to Mr. Dennis A. Woodford of Manitoba Hydro for helpful information and discussion on the Dorsey Auto-transformer.

TABLE OF CONTENTS

Symbols and Abbreviations

ac	Alternating Current
com	Common (winding)
C.T.	Current Transformer
dc	Direct Current
ESP	Earth's Surface Potential
GIC	Geomagnetically-Induced Current
HVDC	High Voltage Direct Current
L.H.S.	Left Hand Side
L-L	Line to Line
L-N	Line to Neutral
P.F.	Power Factor
p.u.	Per Unit
R.H.S.	Right Hand Side
Ser	Series (winding)
SIC	Solar Induced Current
VA	Volt-Ampere
1Ø	Single Phase
3Ø	Three Phase
$\boxed{N}$	Nonlinear Branch (Magnetizing Branch)

CHAPTER 1

INTRODUCTION

It is known that electrons and protons emitted by a solar flare can be captured by the earth's magnetic field, some 20 to 40 hours after the flare occurrence, depending on their initial velocity and trajectory. This phenomenon causes transient fluctuations in the geomagnetic field, having fundamental periods of the order of 5 minutes to 4 hours. These fluctuations are termed "Geomagnetic Storms" and induce voltages in the earth's surface, termed "Earth-Surface Potentials" (ESP's), since the earth's surface is a conductor [1] .

ESP's act as quasi-dc voltages so far as power frequencies (60 or 50 HZ) are concerned, and can produce spurious quasi-dc currents in power systems, termed, "Geomagnetically-Induced Currents" (GIC's) (or sometimes "Solar Induced Currents" (SIC's)) wherever there is a closed path in the system through geographically-remote grounded points. In fact, ESP and hence GIC, are functions of igneous rock geology as well as latitude, and increase with increasing northern latitudes [2] .

GIC's can cause major disturbances in power systems [3] . These effects have recently been more pronounced due to tendency toward relatively longer lines and interconnections. GIC's in excess of 100 amperes have been measured in transformer neutral leads [4] .

One of the configurations that causes GIC in power system to exist is a delta-grounded-wye transformer connected to either side of a transmission line which is grounded at another remote station, as shown in Figure 1 [5] .

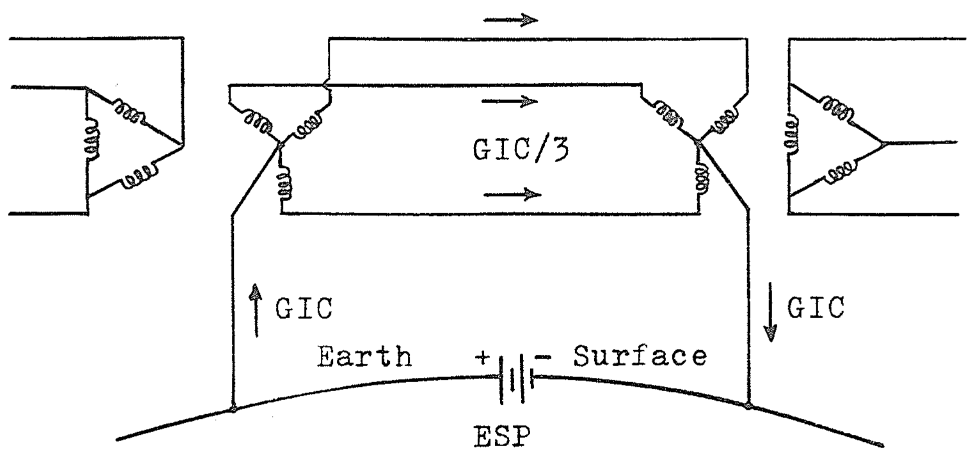

Fig. 1 A Configuration Resulting in GIC's Presence in Power Systems

In such a situation, GIC flows in the transmission line via the transformer neutrals. This current can be many times larger than the RMS value of the ac exciting current of the transformer, and causes simultaneous ac-dc excitation, resulting in half-cycle saturation with a number of associated problems. Among these problems: Production of harmonics, increase of the VAR demand and copper losses, and thus voltage drop in the system as well as change in real power flow, are of utmost importance. There may be several other disturbances in the system, such as relay operation problems, secondary arc current during a single pole switching and effects on HVDC harmonic filters (see Chapter 5).

During the half-cycle saturation, there may be leakage flux spilling outside the normal flux paths within the core, and passing through unlaminated structural steel members, causing excessive localized heating which may cause certain problems such as thermal degradation of the insulation and additional losses [2,4] . This internal heating is highly dependent on the core configuration and is beyond the objectives of this thesis. Thus, it is neglected throughout the calculations.

The main objective of this thesis is to quantitatively determine the behaviour of the transformer with respect to the severity of the GIC. By making use of the results of this study, either directly or indirectly, several other disturbances in power system caused by GIC, and finally the necessity of mitigation of the GIC may be studied and evaluated. These are discussed briefly later in Chapter 5.

To determine the effects of GIC on power transformers and power systems, theoretically and experimentally, several efforts have been made so far [5-7] . In most of these efforts some empirical relationships as well as experimentally evaluated quantities are involved due to complications in analyzing the systems involving non-linear elements. To avoid excessive complication, and to make the analysis feasible, some usual approximations are made, which simplify the analysis substantially. At the same time the resulting errors turn out to be insignificant compared with the degree of simplification. Otherwise, however, the complication makes the analysis impractical, if not impossible.

The method used in this thesis consists in the derivation of the steady-state excitation current and its properties (namely, saturation angle and desaturation angle) under the simultaneous ac-dc excitation (secondary open), using a mathematical model developed for the problem along with a simulation of the magnetizing curve. The magnetizing curve is simulated by straight line segments (see Fig. 9).

The approach is similar to the one employed by Aubin [7] , with some modifications and extension for later uses. Evaluation of the harmonics (including fundamental) is accomplished by making use of Fourier analysis. Then I_{RMS} is calculated using the harmonics as well as direct integration. Then other desired quantities; such as: Copper losses, Iron losses, Var demands, apparent power, active apparent power, true reactive apparent power, distortion power and power factor are calculated and plotted versus GIC . Iron loss is calculated by evaluating the RMS value of the magnetizing voltage. Then the effects of approximations on the results and application of the results in determination of other disturbances in power systems are discussed and finally conclusions are derived.

CHAPTER 2

THEORETICAL ASPECTS

2.1 The Model Developed for the Problem

Referring to Fig. 1, and taking one of the grounded points as voltage reference (the R.H.S. point), the neutral of the other transformer will be at a potential equal to ESP. This voltage, as mentioned previously, acts as a quasi-dc voltage and will be referred to as dc voltage source (K), hereafter. K can be considered as a positive or negative voltage, depending on the location of the grounded points. Throughout this thesis K will be treated as positive, however, it can always be replaced by -K for negative ESP's. If we consider the transformer as an ideal transformer and a non linear magnetizing branch, a dc source will have no effect on the ideal transformer. Unlike the ideal transformer, the non linear branch is affected by the dc voltage. The situation is schematically shown in Fig. 2, where, R_{dc} is the total resistance in the circuit.

On the other hand, the ac source is acting between the neutral of the L.H.S. transformer being at voltage K and the lines. Therefore we arrive at the single phase representation of the sources shown in Fig. 3, where e(t) is the sinusoidal source voltage.

In practice the voltage K cannot be measured (the points on the earth's surface are remote) but is calculated [1]. However, the current produced by this voltage (GIC) can be measured easily (by inserting a dc Ammeter in the neutral lead), and knowing the resistance of the current path, K is easily determined. Having represented the

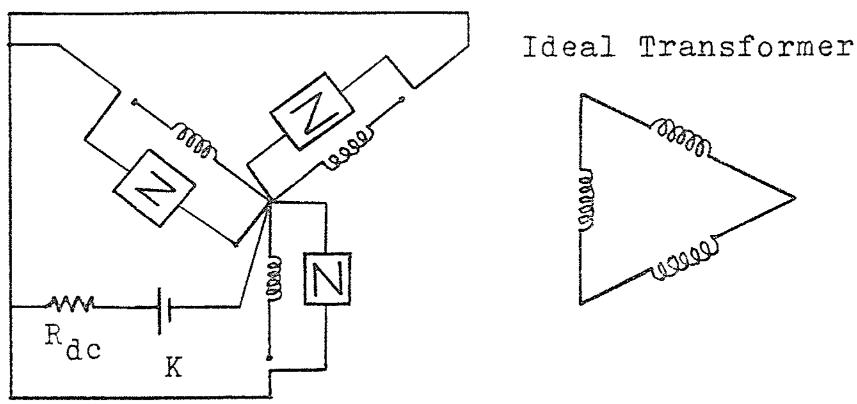

Fig. 2 Effective GIC Representation through the Transformer Magnetizing Branch.

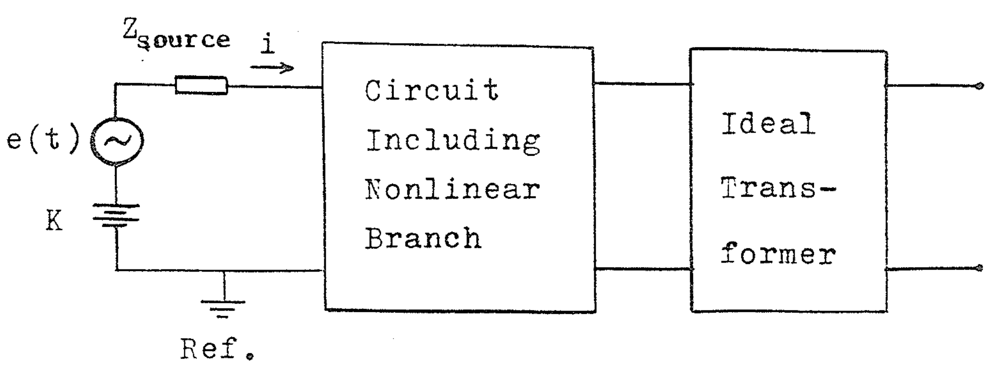

Fig. 3 Single Phase Representation of the Sources according to their effects on the Transformer.

sources according to their effects on the transformer, the usual equivalent circuit of the transformer, shown in Fig. 4, can be used to represent the whole problem as shown in Fig. 5, where,

R_p = series resistance of the transformer Primary.

L_p = Leakage inductance of the transformer Primary.

R_s = Series resistance of the transformer Secondary.

L_s = Leakage inductance of the transformer Secondary.

R = Sum of R_p and the source resistance (or any other series resistance in the circuit).

L_1 = Sum of L_p and the source inductance (or any other series inductance in the circuit).

R_s' = R_s referred to Primary side.

L_s' = L_s referred to Primary side.

R_m = Resistance indicating iron losses.

$\overline{L}$ = The non-linear element characterized by saturation curve.

E = RMS value of the sinusoidal source, and

ω = radian frequency ($2\pi 60$ or $2\pi 50$).

The non linear branch in Fig. 4 has a familiar characteristic; namely, magnetizing curve with hysteresis, as shown in Fig. 6. This curve shows the variation of flux against the magnetizing current and is available for any given transformer.

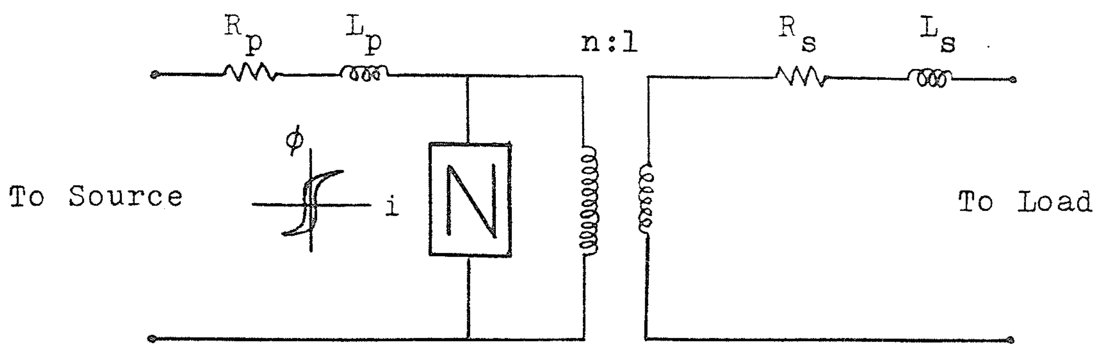

Fig. 4 Usual equivalent circuit of the transformer.

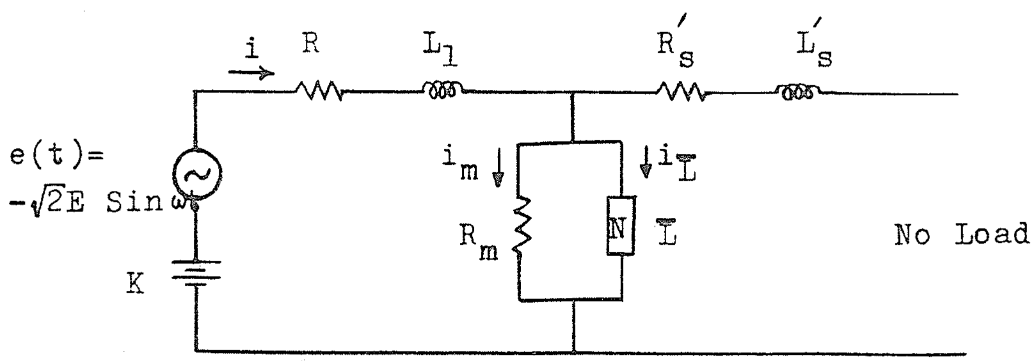

Fig. 5 The representation of the whole problem.

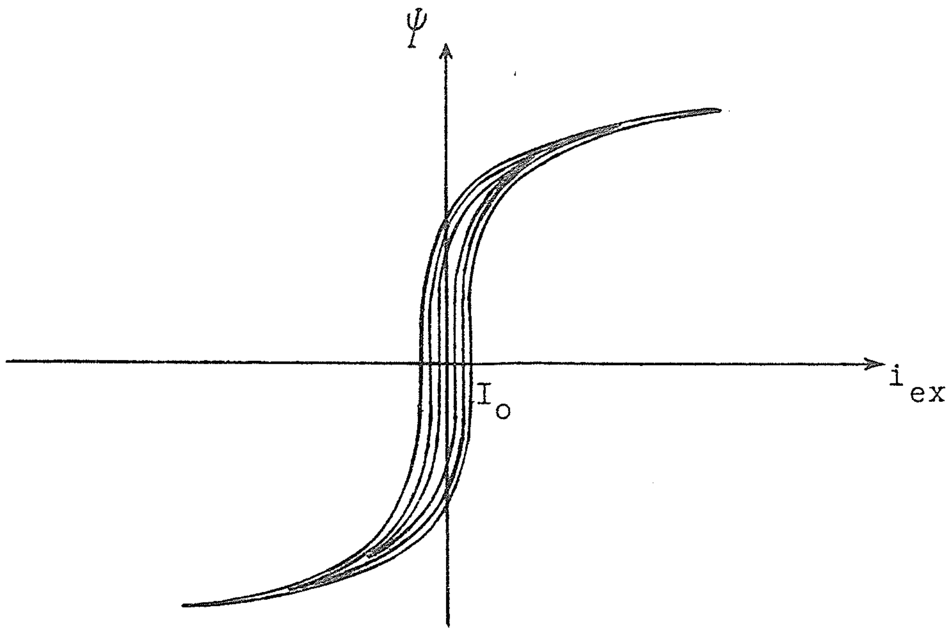

Fig. 6   Magnetizing curve with hysteresis.

To obtain R_m , the current I_o (at $\psi = 0$) is evaluated. At this point the voltage applied to the core has its maximum value (V_o) . Thus, $R_m = \frac{V_o}{I_o}$.

Therefore the characteristic of $\overline{L}$ can be described by magnetizing curve without hysteresis, as shown in Fig. 7.

The magnetizing curve of Fig. 7 (without hysteresis) is obtained by joining the peaks of the various hysteresis curves shown in Fig. 6.

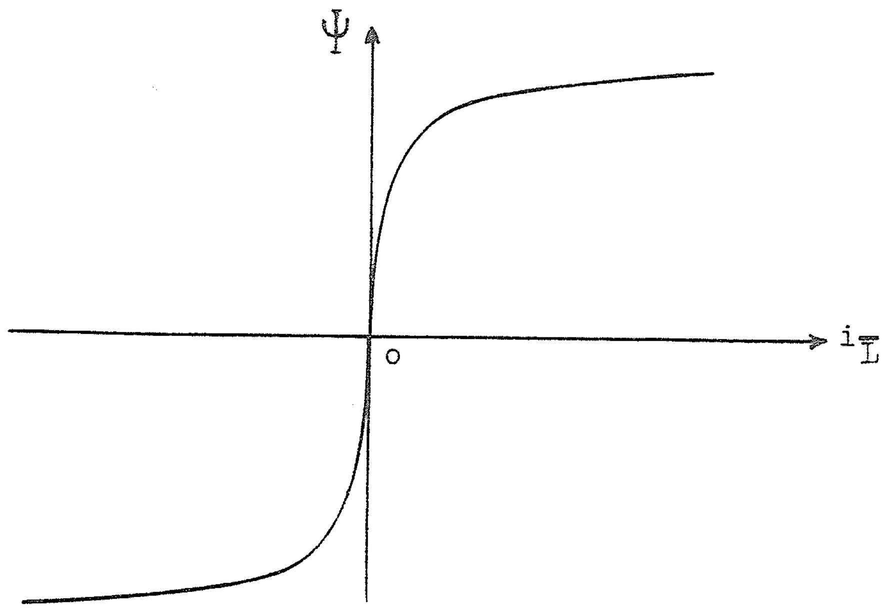

Fig. 7 Magnetizing curve without hysteresis.

R_m is more or less constant and has a large value. This means that the contribution of i_m (shown in Fig. 5) to the exciting current i is negligible. Thus this portion of current, flowing in the series impedance, will not materially modify the voltage applied to the core. Therefore R_m is neglected in evaluating the exciting current (hence $i = i_L$). However, it is used in the calculation of the iron losses.

Power transformers are designed to operate at nominal voltage within the specified limits of the core saturation. Referring to Fig. 7, between these limits the slope of the curve is almost constant and has a very large value, which means very small magnetizing current at normal operation (i.e., on the order of 1% of the nominal current). After saturation, again the curve has almost constant slope but is relatively low, which is approximately the "air core" inductance with the iron core removed. In other words the curve is fairly linear except around the knee, and thus can be approximated by line segments, as shown in Fig. 8, where ϕ_s is the saturation flux.

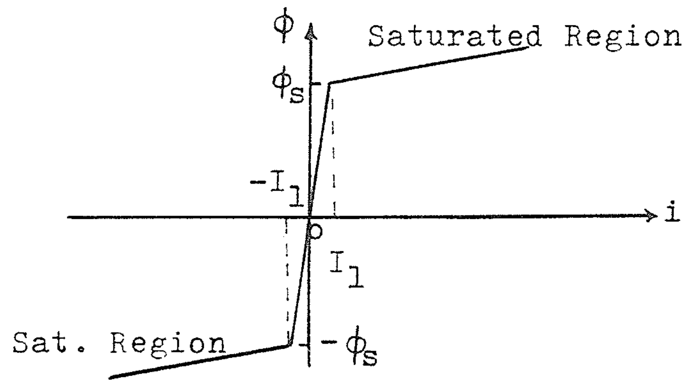

Fig. 8 Approximation of magnetizing curve with line segments.

By neglecting the small amount of magnetizing current in unsaturated region we arrive at the idealized saturation curve of Fig. 9.

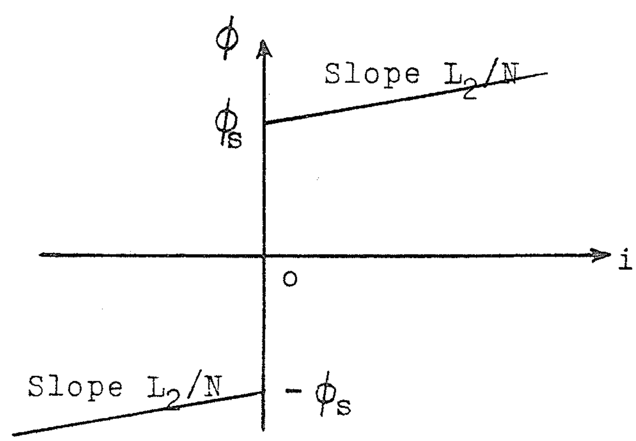

Fig. 9 Idealized saturation curve.

This curve is then used in this thesis to simulate the actual one. The effects of the above idealization are discussed in Chapter 4.

According to Fig. 9, $\overline{L}$ is simulated by the following relationship

$$\overline{L} = \begin{cases} \infty & |\phi| < \phi_s \\ L_2 & |\phi| > \phi_s \end{cases}$$

where, L_2 is approximately the air core inductance of the transformer in question. With no load in secondary, R_s' and L_s' have no effect whatsoever. Therefore the final simplified circuit in single phase representation is as shown in Fig. 10, where, $L = L_1 + L_2$.

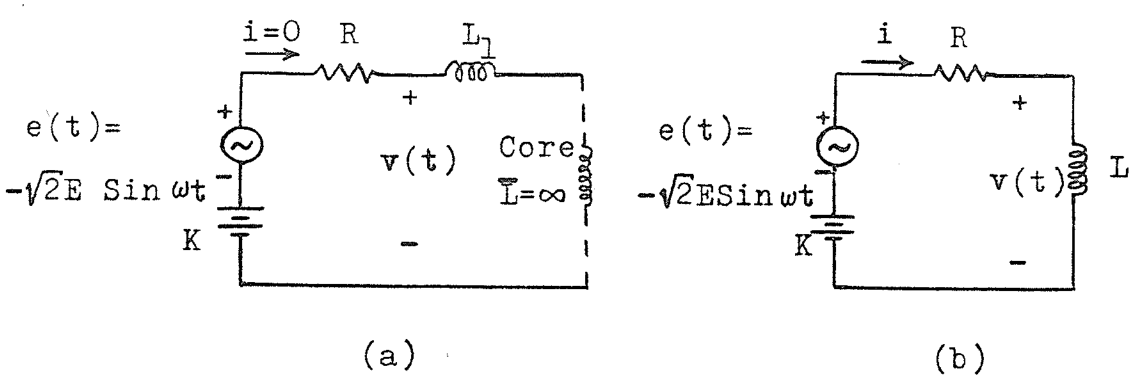

Fig. 10 Final simplified circuit for the problem.
(a) circuit for unsaturated region.
(b) circuit for saturated region.

It must be noted that the direct current does not necessarily have to flow in the winding on which the transformer is excited. Thus, the circuits of Fig. 10 hold for either transformer in Fig. 1.

2.2 Flux Change and the Exciting Current

The exciting current, at first, is similar to the transformer inrush current [8,9] . The inrush current, which has a direct current component, decays and reaches a steady-state current with a zero average, since there is no dc source to maintain the dc component, and the average flux at steady-state is zero. But if there is a dc source in the circuit, it will maintain the dc component and the exciting current will reach a steady-state current with a non-zero average, when the average flux reaches a constant value.

Assume $e = -\sqrt{2}E \sin \omega t$, the circuit is closed at $\omega t = -180^{\circ}$, and at this instant the residual flux in the core is ϕ_r lines and is positive. This will impress a full half-cycle of positive voltage on the circuit and will result in the maximum value of current flowing [10] . As the steady-state current depends on the average flux that will establish itself in the core, these assumptions will not affect the steady-state current and are made for convenience only. In fact, the point, $e = 0$ where $\frac{de}{dt} < 0$ $(t = 0)$, is taken as reference (see Fig. 11).

In the unsaturated region the circuit of Fig. 10(a) applies and obviously $i = 0$. The flux in the core changes in accordance with the applied voltage

$$N\left(\frac{d\phi}{dt}\right) \times 10^{-8} = K - \sqrt{2}E \sin \omega t \quad \text{volts} \tag{1}$$

where, N is the number of winding turns.

Integrating equation (1) and applying initial condition, $\phi = \phi_r$ at $\omega t = -180^{o}$, the flux equation becomes:

$$\phi = \phi_m(1 + \cos \omega t) + \frac{10^8 K}{N\omega}(\omega t - \pi) + \phi_r \quad \text{lines} \tag{2}$$

where, $\phi_m = \sqrt{2}E\ 10^8/N\omega$ lines.

The corresponding flux densities in the iron are:

$$B = B_m(1 + \cos \omega t) + \frac{10^8 K}{N\omega\ A_c}(\omega t - \pi) + B_r \quad \text{gauss} \tag{3}$$

where, B, B_m and B_r are: flux density, peak flux density and residual flux density respectively, and A_c is the cross-sectional area of the core.

Fig. 11 shows the applied voltage, the flux density, and the exciting current. Equation (3) applies until saturation occurs at the angle $-\theta_1$ (θ_1 is shown in Fig. 11), when $B = B_s$. B_s is the saturation flux density and corresponds to ϕ_s. Substituting in equation (3), θ_1 (saturation angle) is such an angle that satisfies the following equation:

$$B_m \cos \theta_1 - \frac{10^8 K}{N\omega A_c}\theta_1 = B_s - B_m - B_r + \frac{10^8 K\pi}{N\omega\ A_c} \tag{4}$$

when ωt exceeds $-\theta_1$, the core goes into saturation and the circuit of Fig. 10(b) applies:

$$K - \sqrt{2}E \sin \omega t = Ri + X \frac{di}{d(\omega t)} \tag{5}$$

where $X = \omega L = \omega(L_1 + L_2) = X_1 + X_2$.

The solution of equation (5) for the initial condition $i = 0$ at $\omega t = -\theta_1$ is

$$i(t) = -\frac{\sqrt{2}\,E\,R}{R^2 + X^2}\left[\sin \omega t - \frac{X}{R}\cos \omega t + e^{-\frac{R}{X}(\omega t + \theta_1)}(\sin \theta_1 + \frac{X}{R}\cos \theta_1)\right]$$

$$+ \frac{K}{R}(1 - e^{-\frac{R}{X}(\omega t + \theta_1)}) \qquad \ldots(6)$$

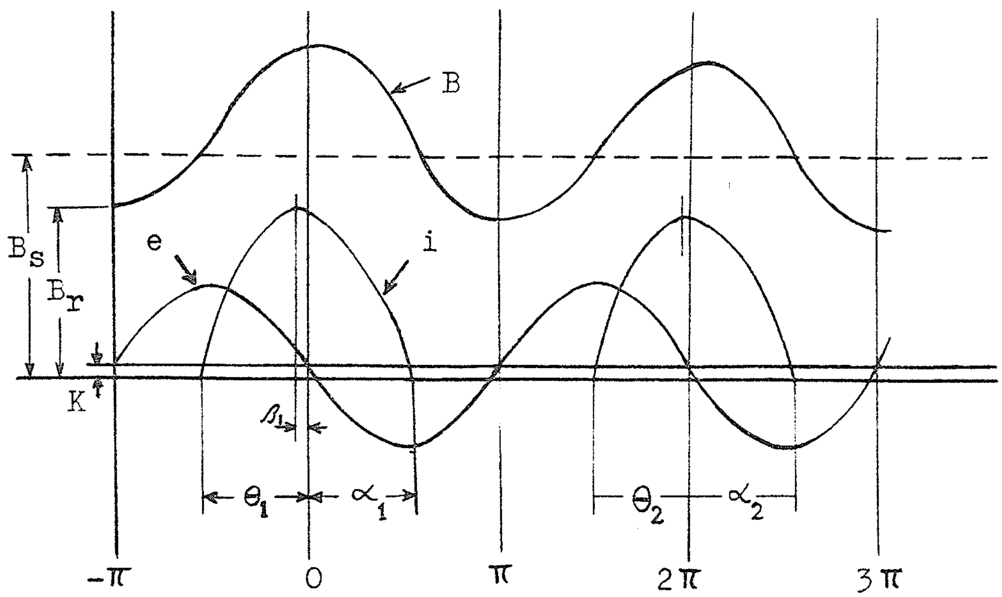

Fig. 11 Applied voltage, current and flux density.

Equation (6) applies until again $B = B_s$ at $\omega t = \alpha_1$. After $\omega t = \alpha_1$ again Fig. 10(a) applies and i remains zero until the next saturation occurs. α_1 (shown in Fig. 10) is such an angle for which i in equation (6) again becomes zero $(\alpha_1 \neq -\theta_1)$.

2.3 Condition for the Steady-State Current

The reduction in the flux at the end of the first cycle due to the series resistance in the circuit (R) is of the following amount [8] ,

$$\Delta\phi_1 = \frac{1}{N\omega}\int_{-\pi}^{\pi} Ri\ d(\omega t) = \frac{R}{N\omega}\int_{-\theta_1}^{\alpha_1} i\ d(\omega t) \qquad (7)$$

where i is defined by equation (6).

This amount is equal to the area under the voltage curve reduced by the Ri component, as shown in Fig. 12.

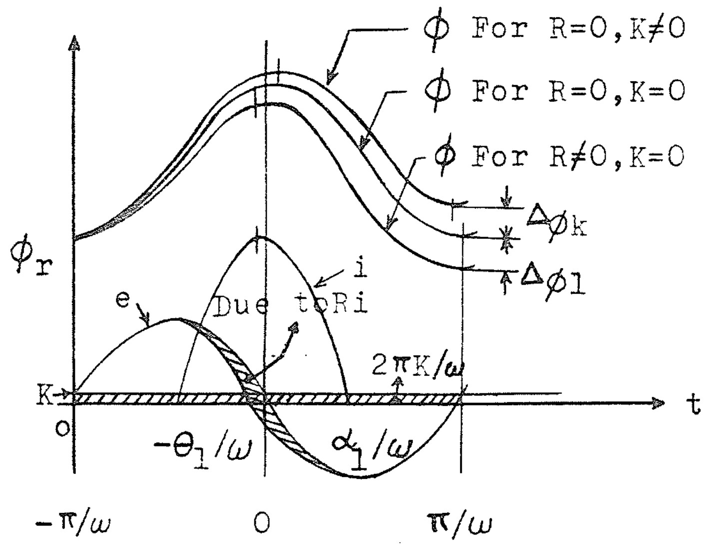

Fig. 12 Reduction and Increase in flux, due to R & K .

Let, after n cycle, θ_n and α_n be the saturation angle and desaturation angle respectively. Then the reduction in the flux due to R, from the beginning to the end of the n^{th} cycle is

$$\Delta\phi_n = \frac{1}{N\omega}\int_{(n-2)\pi}^{n\pi} Ri \; d(\omega t) = \frac{R}{N\omega}\int_{-\theta_n}^{\alpha_n} i \; d(\omega t) \qquad (8)$$

where i is defined by the same equation as before but θ_1 replaced by θ_n (α_1 is also replaced by α_n) .

On the other hand, in each cycle, the flux increases by the following amount due to the dc voltage K ,

$$\Delta\phi_K = \frac{1}{N\omega}\int_{(n-2)\pi}^{n\pi} K \; d(\omega t) = \frac{1}{N\omega}\int_{-\pi}^{\pi} K \; d(\omega t) = \frac{2\pi K}{N\omega} \qquad (9)$$

The current will reach steady state when the flux average remains unchanged, which means

$$R\int_{-\theta}^{\alpha} i \; d(\omega t) = 2\pi K \qquad (10)$$

where, θ and α are steady-state saturation and desaturation angles, and i is defined by equation (6) with θ_1 and α_1 replaced by θ and α . Equation (10) implies that the steady-state current has an average (I_A) equal to $\frac{K}{R}$. The operating point on magnetizing curve does not correspond to this current directly but corresponds to the average steady-state flux in the core.

CHAPTER 3

CALCULATIONS

3.1 The Selected Per Unit Bases

To make the calculations more convenient, and to get rid of additional parameters such as R and E, the following per unit bases are assumed throughout the calculations:

$$\text{Base Voltage}_{(L-N)} = E \quad \text{volts(rms)} \tag{11a}$$

$$\text{Base (VA)}_{1\phi} = \frac{E^2}{R} \tag{11b}$$

Then obviously:

$$\text{Base Impedance} = R \quad \text{ohms} \tag{11c}$$

$$\text{Base Current} = \frac{E}{R} \quad \text{amps(rms)} \tag{11d}$$

$$\text{Base Voltage}_{(L-L)} = \sqrt{3}\,E \quad \text{volts(rms)} \tag{11e}$$

$$\text{Base (VA)}_{3\phi} = \frac{3E^2}{R} \tag{11f}$$

3.2 The Steady-State Current

Integrating equation (5) over the saturated region

$$\int_{-\theta}^{\alpha} (K - \sqrt{2}E \sin \omega t)\, d(\omega t) = \int_{-\theta}^{\alpha} R\, i(\omega t)\, d(\omega t) + \int_{i=0}^{i=0} X\, di \qquad \ldots(12)$$

obviously the last term is zero.

Substituting from equation (10) for the R.H.S. in (12), it results in the following condition for steady state

$$\frac{K}{E} = \sqrt{2}\, \frac{\cos\alpha - \cos\theta}{2\pi - (\alpha + \theta)} \tag{13}$$

Therefore the steady-state exciting current in p.u. is as follows

$$i(\omega t) = -\frac{\sqrt{2}}{1+x^2}\left(\sin \omega t - x\cos \omega t + e^{-\frac{\omega t+\theta}{x}}(\sin\theta + x\cos\theta)\right)$$

$$+ k\left(1 - e^{-\frac{\omega t+\theta}{x}}\right) \text{ p.u.} \quad -\theta \le \omega t \le \alpha \qquad (14a)$$

$$i(\omega t) = 0 \quad \text{for the rest of period} \qquad (14b)$$

where,

$$k = K(\text{p.u.}) = \sqrt{2}\,\frac{\cos\alpha - \cos\theta}{2\pi - (\alpha+\theta)} \quad \text{p.u.} \qquad (14c)$$

$$x = X(\text{p.u.}) = \frac{X}{R} = \frac{\omega(L_1+L_2)}{R} = x_1 + x_2 \quad \text{p.u.} \qquad (14d)$$

and α is defined by $i(\alpha) = 0$.

To find α , the condition $i = 0$ at $\omega t = \alpha$ may be substituted in (14a). Let

$$\gamma = \alpha + \theta \quad (0 < \gamma < 2\pi) \qquad (14e)$$

Then

$$\alpha = \arctan\left\{\left[((1+x^2)(1-\cos\gamma) + x(2\pi-\gamma))e^{\frac{\gamma}{x}} - (1+x^2)(1-\cos\gamma) - (2\pi-\gamma)(\sin\gamma + x\cos\gamma)\right] \Big/ \left[((1+x^2)\sin\gamma + (2\pi-\gamma))e^{\frac{\gamma}{x}} - (1+x^2)\sin\gamma + (2\pi-\gamma)(x\sin\gamma - \cos\gamma)\right]\right\} \qquad (14f)$$

As was mentioned before, the initial conditions at the switching instant do not affect the steady-state current. Therefore the steady-state currents of all three phases have the same shape defined by equation (14a) through (14f) but 120^{0} phase difference from one another, according to the phase sequence of the sinusoidal input voltage.

3.3 The Exciting Current After Complete Saturation

For $0 < \gamma < 2\pi$ the core is saturated only for $\frac{\gamma}{\omega}$ seconds and for the rest of period remains unsaturated $(i = 0)$. When $\gamma = 2\pi$, it changes from partial saturation to complete saturation $(\frac{\gamma}{\omega} = \frac{2\pi}{\omega} = T)$. The value of k at this change is calculated as follows:

$$k = \sqrt{2}\,\frac{\cos\alpha - \cos(\gamma - \alpha)}{2\pi - \gamma}$$

$$= \sqrt{2}\,\sin\left(\frac{\gamma}{2} - \alpha\right)\frac{\sin(\pi - \frac{\gamma}{2})}{\pi - \frac{\gamma}{2}}$$

as γ approaches 2π,

$$k_c = \lim_{\gamma \to 2\pi} k = \sqrt{2}\,\sin(\pi - \alpha) = \sqrt{2}\,\sin\alpha$$

Substituting $i = 0$, $\omega t = \alpha$, $\theta = 2\pi - \alpha$, $k = \sqrt{2}\,\sin\alpha$ in equation (14a)

$$\tan\alpha = -\frac{1}{x}$$

or

$$\sin\alpha = \frac{1}{\sqrt{1 + x^2}} \qquad (\sin\alpha \text{ is positive since } k > 0)$$

Thus

$$k_c = \sqrt{2}\,\sin\alpha = \frac{\sqrt{2}}{\sqrt{1 + x^2}} \tag{15}$$

For $k \geq k_c$, the core remains completely in saturation and the circuit of Fig. 10(b) applies for the whole period. Therefore

$$i(\omega t) = -\frac{\sqrt{2}}{1+x^2}(\sin\omega t - x\cos\omega t) + k$$

$$= -\frac{\sqrt{2}}{\sqrt{1+x^2}}\sin(\omega t - \tan^{-1}x) + k \qquad k \geq k_c$$

$$\ldots(16)$$

Obviously equations (14a) through (14f) hold for $0 \leq k \leq k_c$. For $k = 0$, $i(\omega t) = 0$ for the whole period, which indicates no saturation under normal operation (no GIC) .

3.4 Harmonics

Calculation of harmonics is accomplished by using a Fourier analysis as follows:

$i(\omega t)$ may be expressed as

$$i(\omega t) = -\sqrt{2}\sum_{m=1}^{\infty} I_{Rm}\sin m\,\omega t + \sqrt{2}\sum_{m=1}^{\infty} I_{xm}\cos m\omega t + I_A$$

$$= -\sqrt{2}\sum_{m=1}^{\infty} I_m \sin(m\,\omega t - \phi_m) + I_A \qquad \text{p.u.} \qquad (17)$$

where,

I_{Rm} = RMS value of the real component (in phase with the voltage $e(t)$) of the m^{th} harmonic.

I_{xm} = RMS value of the reactive component (90^o lagging the voltage $e(t)$) of the m^{th} harmonic.

I_m = RMS value of the m^{th} harmonic.

ϕ_m = The phase angle of the m^{th} harmonic.

I_A = Average of $i(\omega t)$ (dc component).

Then,

$$I_{Rn} = -\frac{1}{\sqrt{2}\pi}\int_{-\theta}^{\alpha} i(\omega t)\sin n\omega t\, d(\omega t) \qquad \text{p.u.} \qquad (18a)$$

$$I_{xn} = \frac{1}{\sqrt{2}\pi}\int_{-\theta}^{\alpha} i(\omega t)\cos n\,\omega t\, d(\omega t) \qquad \text{p.u.} \qquad (18b)$$

$$I_A = \frac{1}{2\pi}\int_{-\theta}^{\alpha} i(\omega t)\; d(\omega t) = k \qquad \text{p.u.} \qquad (18c)$$

$$I_n = \sqrt{I_{Rn}^2 + I_{xn}^2} \qquad \text{p.u.} \qquad (18d)$$

$$\phi_n = \tan^{-1}(I_{xn}/I_{Rn}) \qquad (18e)$$

where, $i(\omega t)$ is defined by equations (14a) through (14f) for

$k < \frac{\sqrt{2}}{\sqrt{1+x^2}}$ and by equation (16) for $k \geq \frac{\sqrt{2}}{\sqrt{1+x^2}}$.

Performing the above integrals:

for $n = 1$ (fundamental)

$$I_{R1} = \frac{\alpha+\theta}{2\pi(1+x^2)} - \frac{\sin 2\alpha + \sin 2\theta}{4\pi(1+x^2)} + \frac{x(\cos 2\alpha - \cos 2\theta)}{4\pi(1+x^2)}$$

$$+ \frac{x}{\pi(1+x^2)}\left(\frac{k}{\sqrt{2}} + \frac{\sin\theta + x\cos\theta}{1+x^2}\right)(x\cos\theta - \sin\theta$$

$$- (x\cos\alpha + \sin\alpha)e^{-\frac{\alpha+\theta}{x}}) + \frac{k}{\sqrt{2}\pi}(\cos\alpha - \cos\theta) \qquad \text{p.u.}$$

$$k < k_c \qquad (19a)$$

$$I_{R1} = \frac{1}{1+x^2} \qquad \text{p.u.} \qquad k \geq k_c \qquad (19b)$$

and

$$I_{x1} = \frac{x(\alpha + \theta)}{2\pi(1 + x^2)} + \frac{x(\sin 2\alpha + \sin 2\theta)}{4\pi(1 + x^2)} + \frac{\cos 2\alpha - \cos 2\theta}{4\pi(1 + x^2)}$$

$$- \frac{x}{\pi(1 + x^2)} \left(\frac{k}{\sqrt{2}} + \frac{\sin\theta + x\cos\theta}{1 + x^2} \right)(x\sin\theta + \cos\theta$$

$$+ (x\sin\alpha - \cos\alpha)e^{-\frac{\alpha+\theta}{x}}) + \frac{k}{\sqrt{2}\pi}(\sin\alpha + \sin\theta) \quad \text{p.u.}$$

$$k < k_c \qquad (20a)$$

$$I_{x1} = \frac{x}{1 + x^2} \quad \text{p.u.} \qquad k \geq k_c \qquad (20b)$$

and

$$I_1 = \sqrt{I_{R1}^2 + I_{x1}^2} \quad (I_{R1} \text{ from (19a) and } I_{x1} \text{ from (20a)}) \text{ p.u.}$$

$$k < k_c \qquad (21a)$$

$$I_1 = \frac{1}{\sqrt{1 + x^2}} \quad \text{p.u.} \qquad k \geq k_c \qquad (21b)$$

I_{R1} , I_{x1} and I_1 are plotted versus k and for different x , in Fig. 13, 14 and 15, respectively.

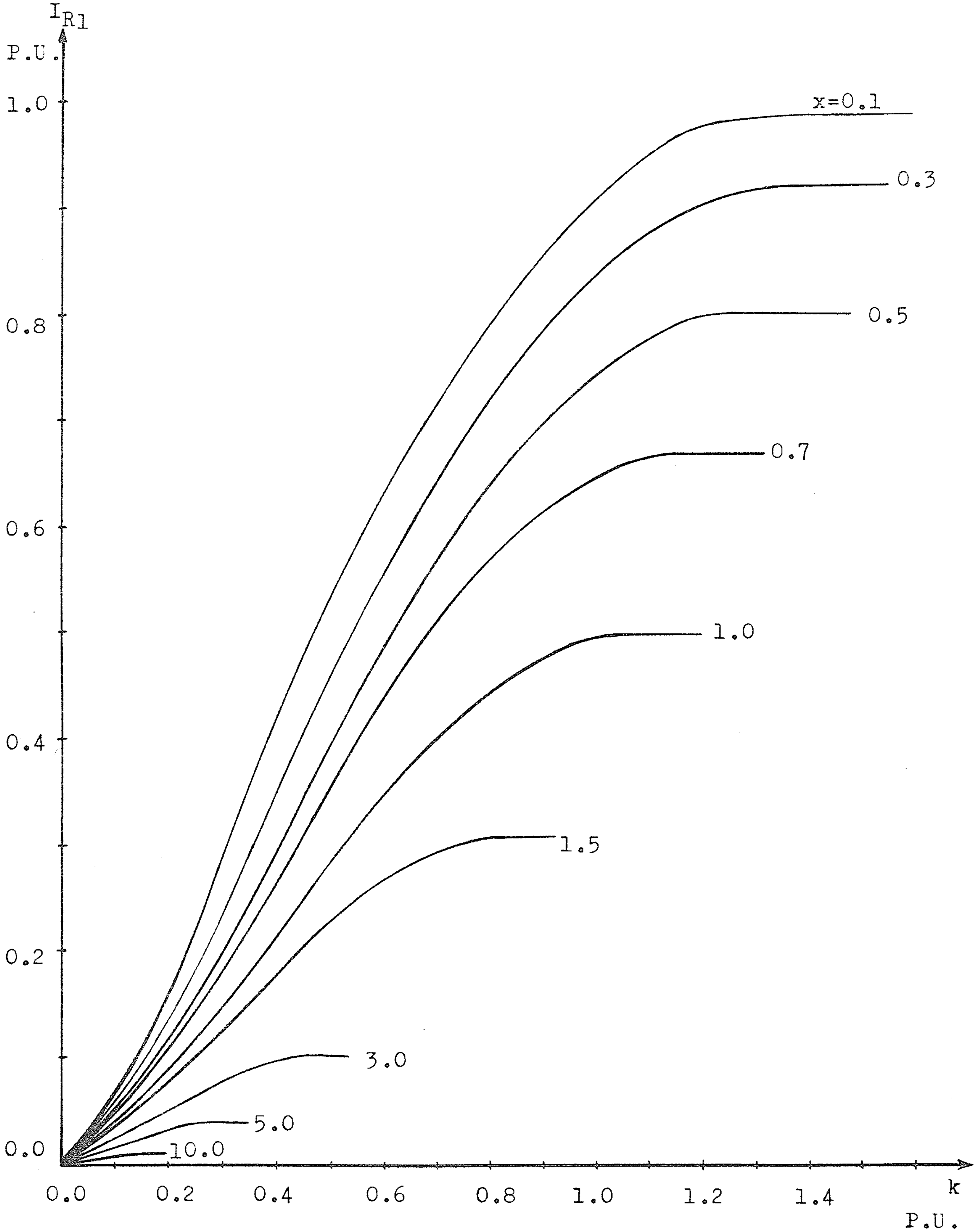

Fig. 13-Real Component Of Fundamental Frequency.

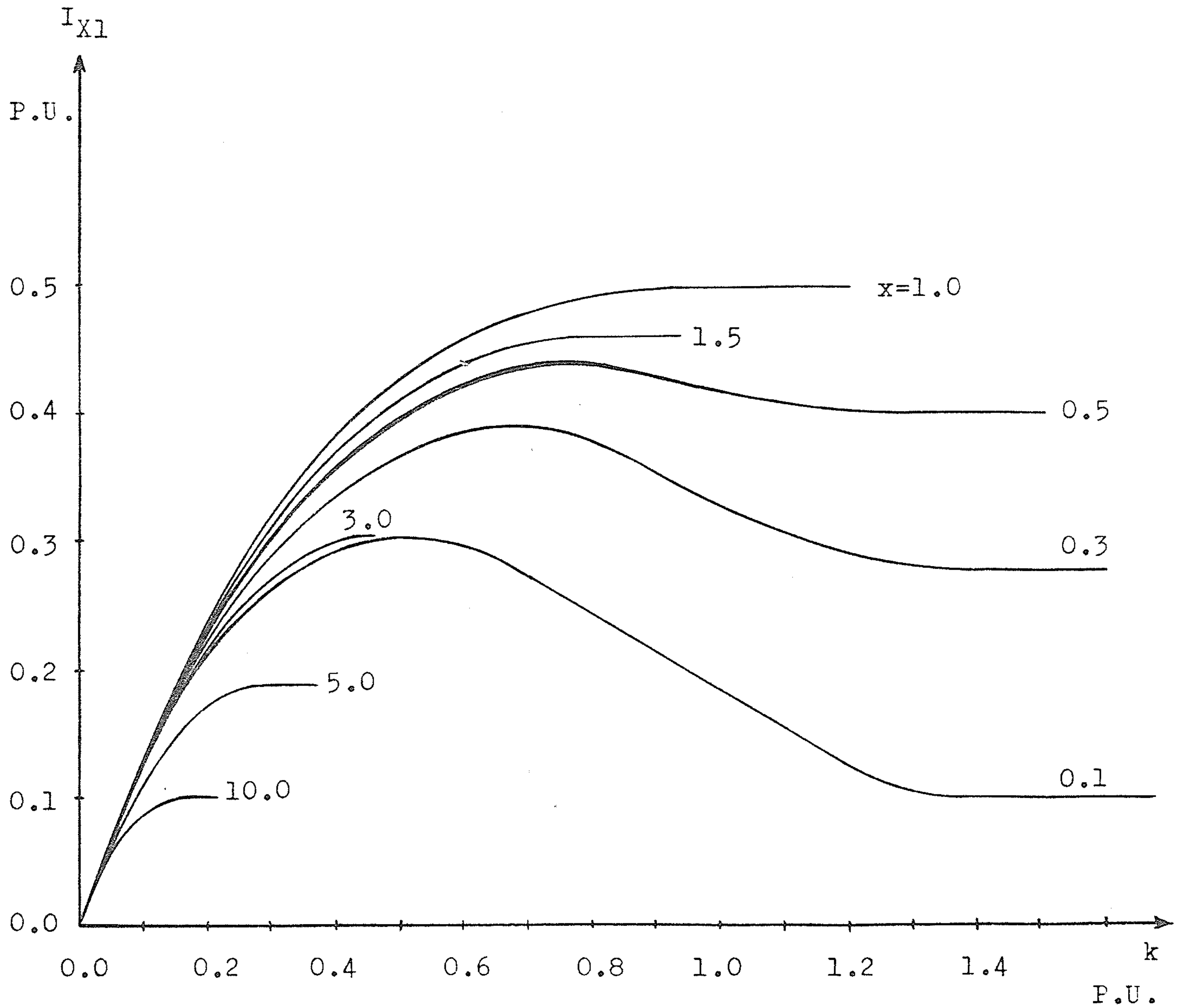

Fig. 14- Reactive Component Of fundamental Frequency.

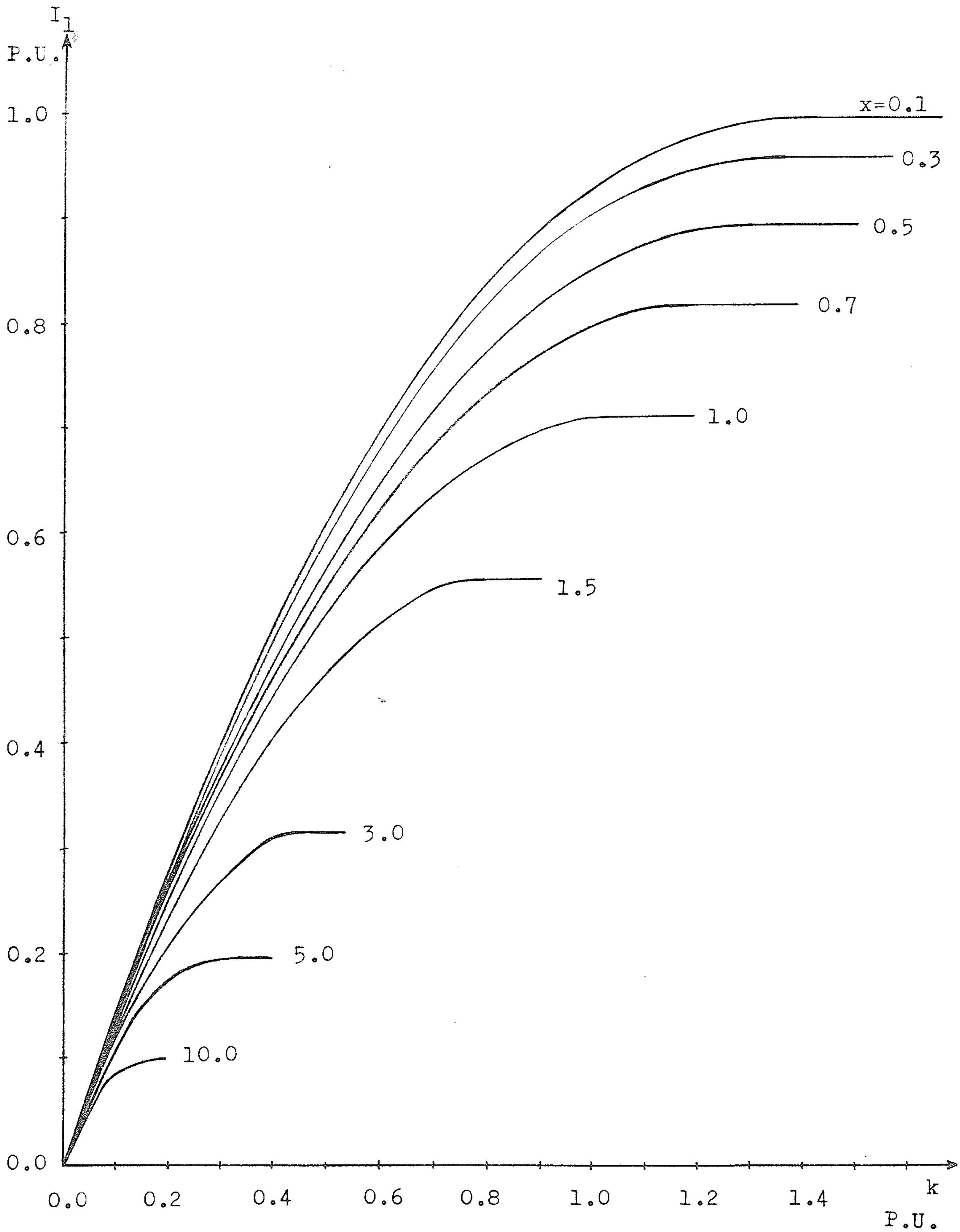

Fig. 15 - Fundamental RMS .

For $n = 2, 3, 4, \ldots$ (harmonics)

$$I_{Rn} = \frac{1}{2\pi(1+x^2)(n+1)} \left(- \sin(n+1)\alpha - \sin(n+1)\theta + x(\cos(n+1)\alpha - \cos(n+1)\theta)\right)$$

$$+ \frac{1}{2\pi(1+x^2)(n-1)} \left(\sin(n-1)\alpha + \sin(n-1)\theta + x(\cos(n-1)\alpha - \cos(n-1)\theta) \right)$$

$$+ \frac{x}{\pi(1+n^2x^2)} \left(\frac{k}{\sqrt{2}} + \frac{\sin\theta + x\cos\theta}{1+x^2}\right)\left(nx\cos n\theta - \sin n\theta\right.$$

$$\left. - (nx\cos n\alpha + \sin n\alpha)e^{-\frac{\alpha+\theta}{x}} \right) + \frac{k}{\sqrt{2}\,\pi\, n}(\cos n\alpha - \cos n\theta) \quad \text{p.u.}$$

$$k < k_c \qquad (22a)$$

$$I_{Rn} = 0 \qquad k \geq k_c \qquad (22b)$$

and

$$I_{xn} = \frac{1}{2\pi(1+x^2)(n+1)} \left(\cos(n+1)\alpha - \cos(n+1)\theta + x(\sin(n+1)\alpha + \sin(n+1)\theta)\right)$$

$$+ \frac{1}{2\pi(1+x^2)(n-1)} \left(-\cos(n-1)\alpha + \cos(n-1)\theta + x(\sin(n-1)\alpha + \sin(n-1)\theta)\right)$$

$$- \frac{x}{\pi(1+n^2x^2)} \left(\frac{k}{\sqrt{2}} + \frac{\sin\theta + x\cos\theta}{1+x^2}\right)\left(nx\sin n\theta + \cos n\theta\right.$$

$$\left. + (nx\sin n\alpha - \cos n\alpha)e^{-\frac{\alpha+\theta}{x}} \right) + \frac{k}{\sqrt{2}\pi\, n}(\sin n\alpha + \sin n\theta) \quad \text{p.u.}$$

$$k < k_c \qquad (23a)$$

$$I_{xn} = 0 \qquad k \geq k_c \qquad (23b)$$

and

$$I_n = \sqrt{I_{Rn}^2 + I_{xn}^2} \quad (I_{Rn} \text{ from (22a) and } I_{xn} \text{ from (23a)) p.u.}$$

$$k < k_c \qquad (24a)$$

$$I_n = 0 \qquad\qquad k \geq k_c \qquad (24b)$$

The second through the fifth harmonic (in per unit of fundamental) are plotted versus k and for different x, in Fig. 16, 17, 18 and 19, respectively. The higher order harmonics are negligible.

3.5 Effective Current

The RMS value of the current is defined as follows

$$I^2_{RMS} = \frac{1}{2\pi} \int_{-\theta}^{\alpha} [i(\omega t)]^2 \, d(\omega t) \qquad \text{p.u.} \qquad (25)$$

where, $i(\ t)$ is given by equation (14a) through (14f) for $k < \dfrac{\sqrt{2}}{\sqrt{1+x^2}}$, and by equation (16) for $k \geq \dfrac{\sqrt{2}}{\sqrt{1+x^2}}$.

Performing the above integral results in

$$\begin{aligned} I^2_{RMS} = {} & \left(k^2 + \frac{1}{1+x^2}\right)\left(\frac{\alpha+\theta}{2\pi}\right) + \frac{(x^2-1)(\sin 2\alpha + \sin 2\theta)}{4\pi(1+x^2)^2} \\ & + \frac{x(\cos 2\alpha - \cos 2\theta)}{2\pi(1+x^2)^2} + \frac{x}{4\pi}\left(k + \frac{\sqrt{2}}{1+x^2}(\sin\theta + x\cos\theta)\right)^2 \\ & \left(1 - e^{-\frac{2(\alpha+\theta)}{x}}\right) + \frac{\sqrt{2}\,k}{\pi(1+x^2)}(\cos\alpha + x\sin\alpha - \cos\theta + x\sin\theta) \\ & - \frac{kx}{\pi}\left(k + \frac{\sqrt{2}}{1+x^2}(\sin\theta + x\cos\theta)\right)\left(1 - e^{-\frac{\alpha+\theta}{x}}\right) \\ & - \frac{x\sqrt{2}}{\pi(1+x^2)}\left(k + \frac{\sqrt{2}}{1+x^2}(\sin\theta + x\cos\theta)\right)\left((\sin\alpha)e^{-\frac{\alpha+\theta}{x}} + \sin\theta\right) \end{aligned}$$

$$\text{p.u.} \quad k < k_c \qquad \ldots(26a)$$

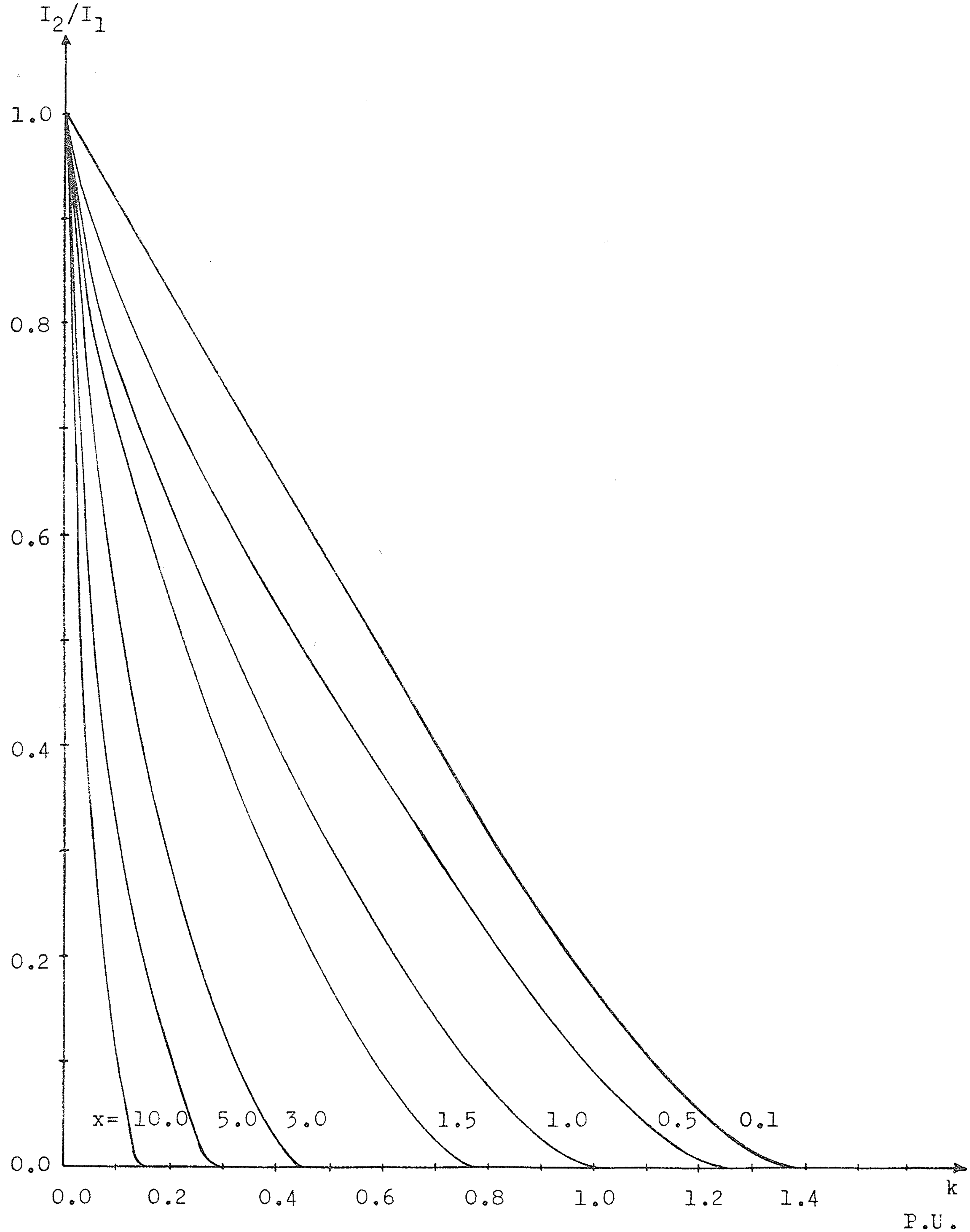

Fig. 16– Second Harmonic In Per Unit Of Fundamental.

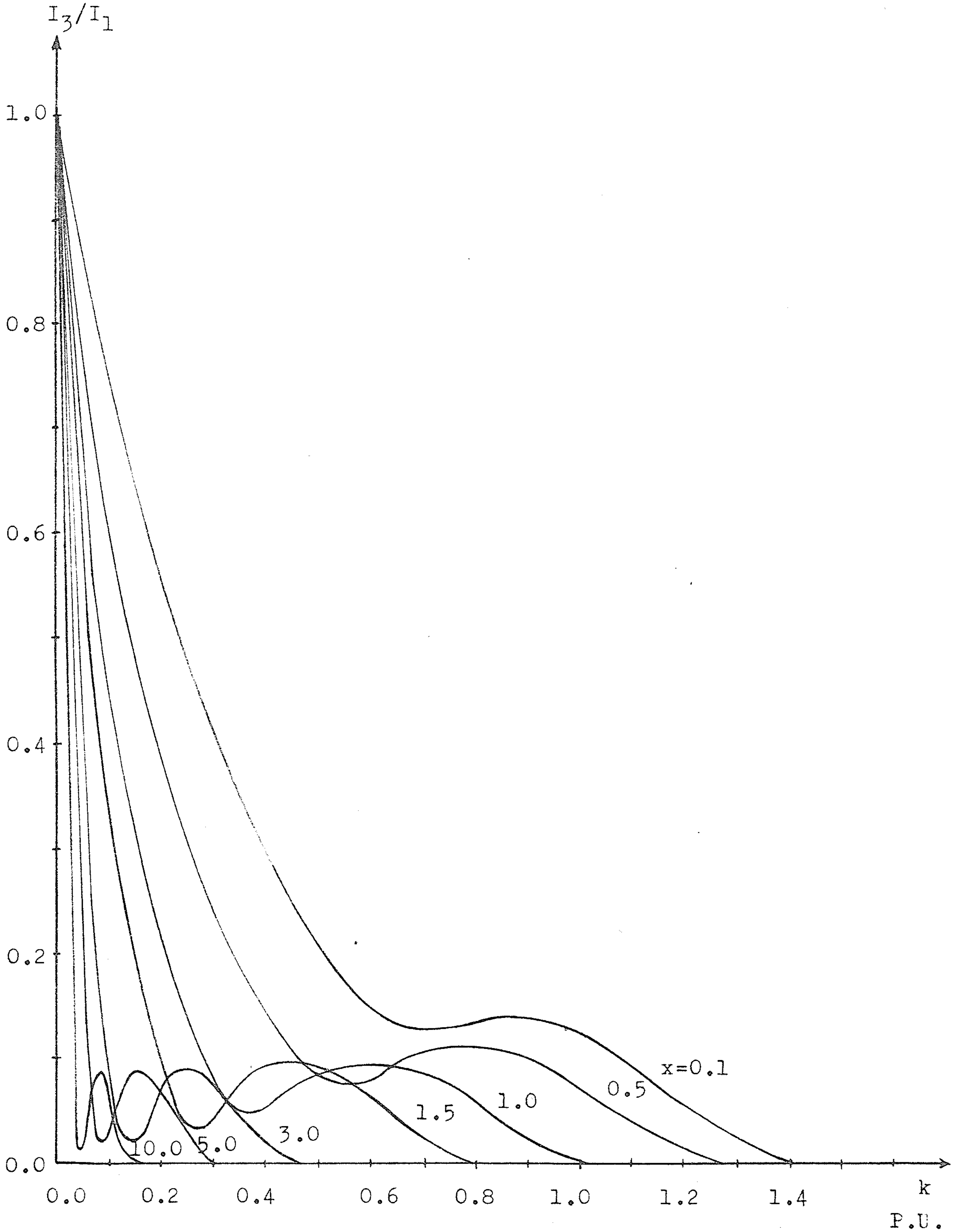

Fig. 17- Third Harmonic In Per Unit Of Fundamental.

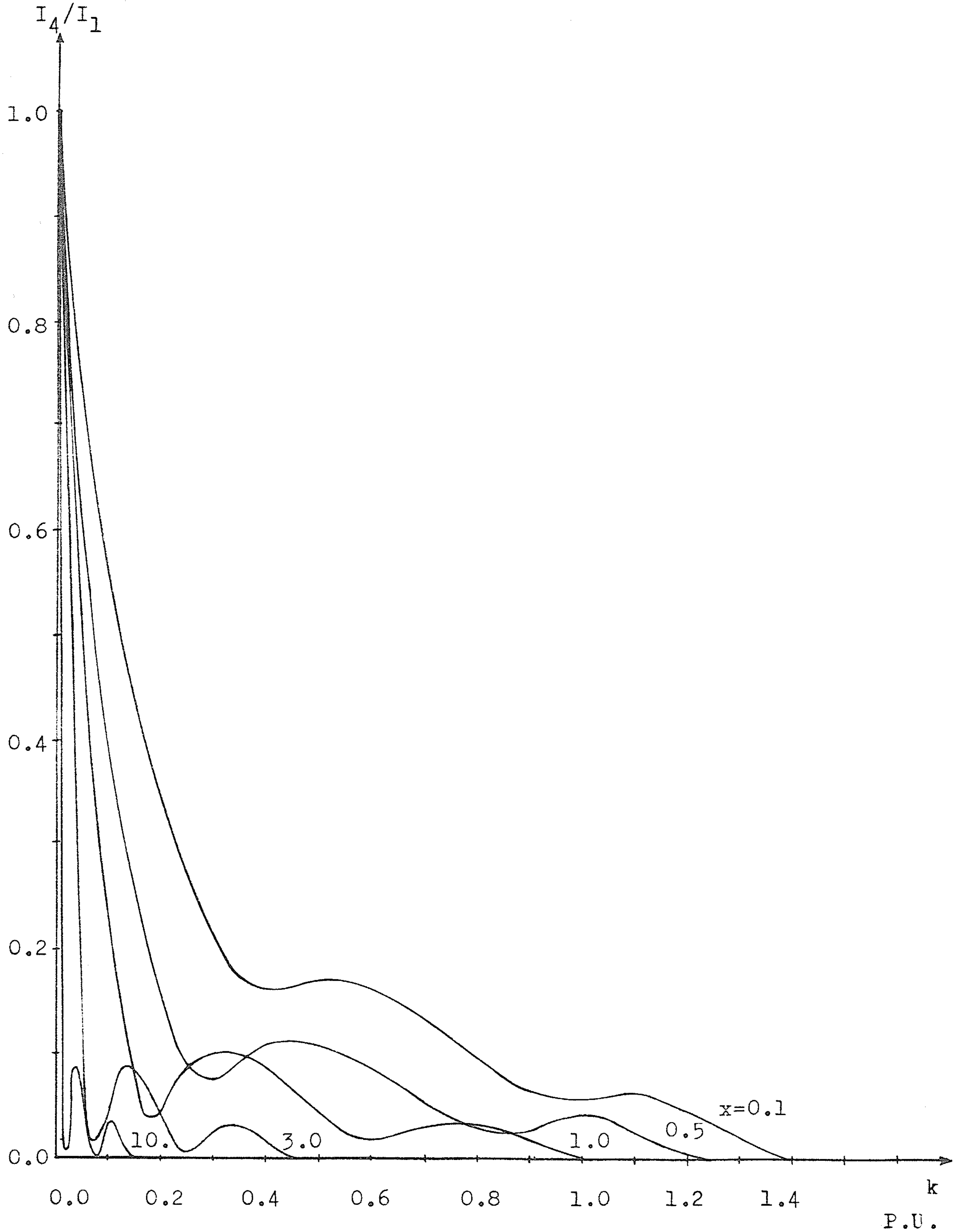

Fig. 18 - 4th Harmonic In Per Unit Of Fundamental.

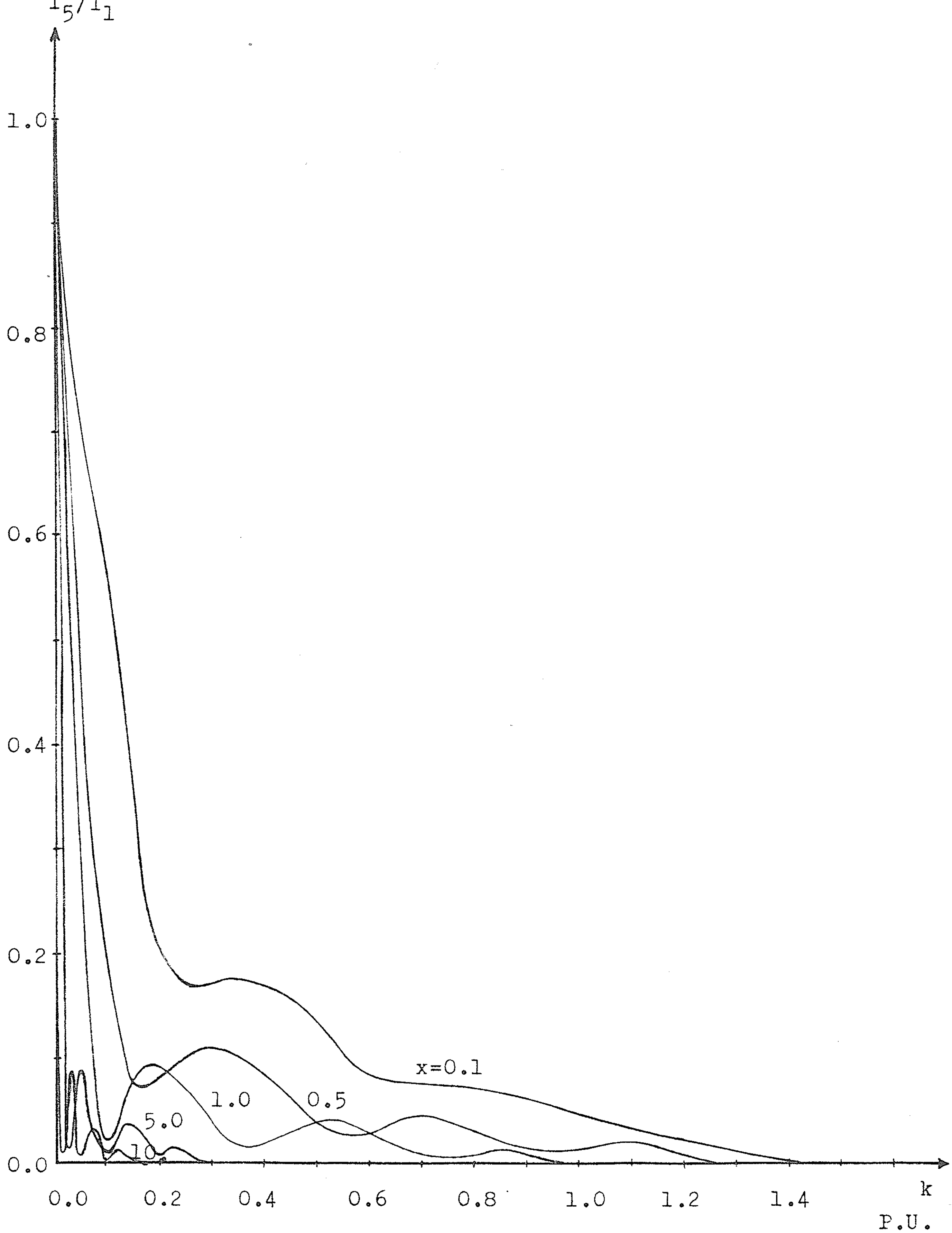

Fig. 19 - 5th Harmonic In Per Unit Of Fundamental.

$$I_{RMS}^2 = k^2 + \frac{1}{1 + x^2} \quad \text{p.u.} \qquad k \geq k_c \qquad (26b)$$

I_{RMS} is plotted versus k and for different x , in Fig. 20.

On the other hand I_{RMS} can be expressed as follows

$$I_{RMS}^2 = I_A^2 + \sum_{n=1}^{\infty} I_n^2 \cong I_A^2 + \sum_{n=1}^{5} I_n^2 \qquad (27)$$

where I_A and I_n are given in previous section.

Computation of I_{RMS} by equation (27) showed insignificant difference from that of equation (26a).

3.6 Copper Loss

Copper loss is the average real power in the series resistance (R) , and is defined by the following relationship

$$P_c = \frac{1}{2\pi} \int_{-\pi}^{\pi} R\, i^2\, d(\omega t) = R\, I_{RMS}^2 \quad \text{watts/Phase} \qquad (28)$$

and in p.u.,

$$P_c = I_{RMS}^2 \cong k^2 + \sum_{n=1}^{5} I_n^2 \quad \text{p.u.} \qquad (29)$$

where I_{RMS} is given by equations (26a) and (26b).

Obviously P_c for 3 phase in p.u. is the same as equation (29).
P_c is plotted versus k and for different x , in Fig. 21.
If R is R_p plus source resistance then the copper loss in transformer is $R_p I_{RMS}^2 = R_p P_c$ (p.u.) .

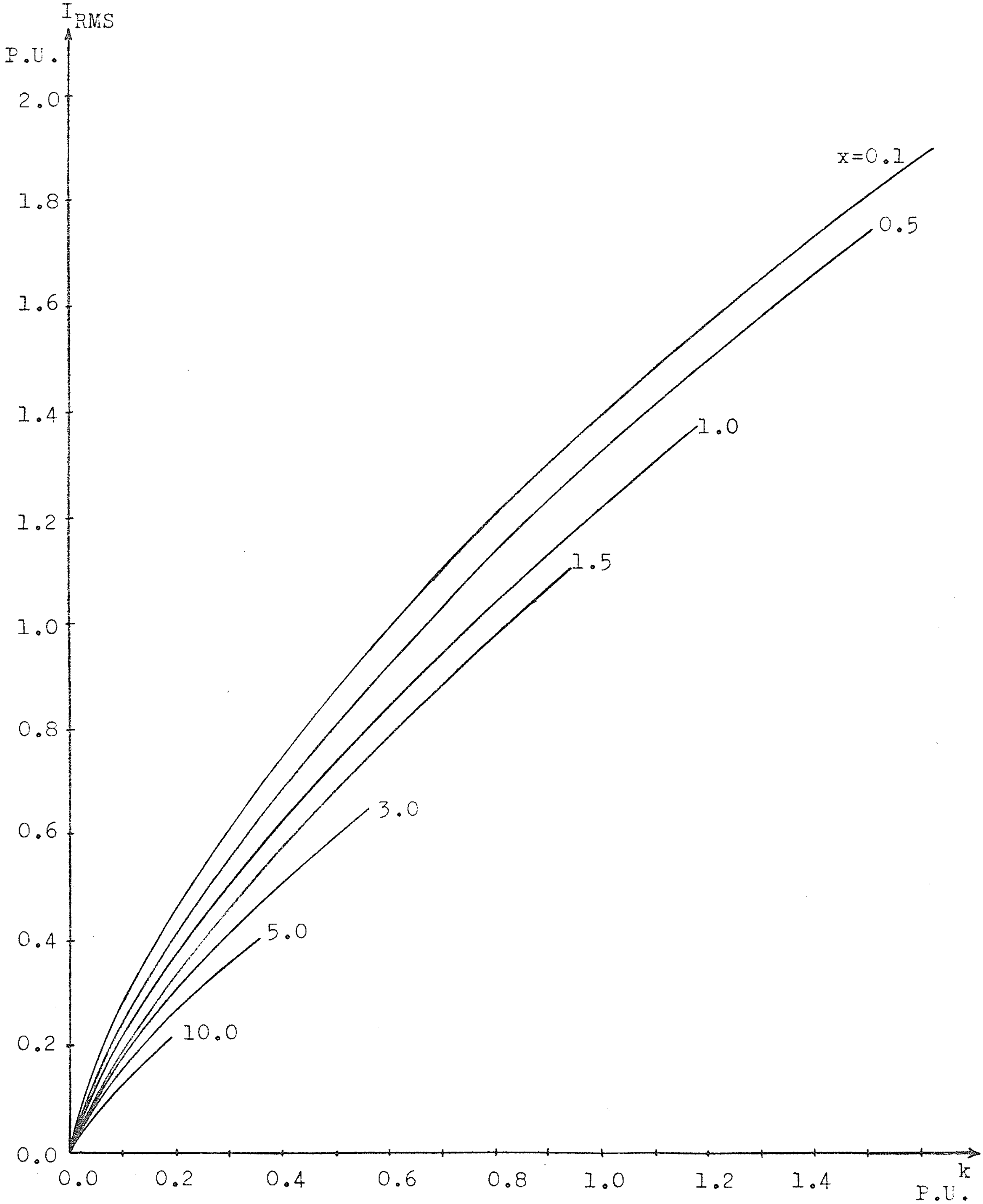

Fig. 20- Effective Current .

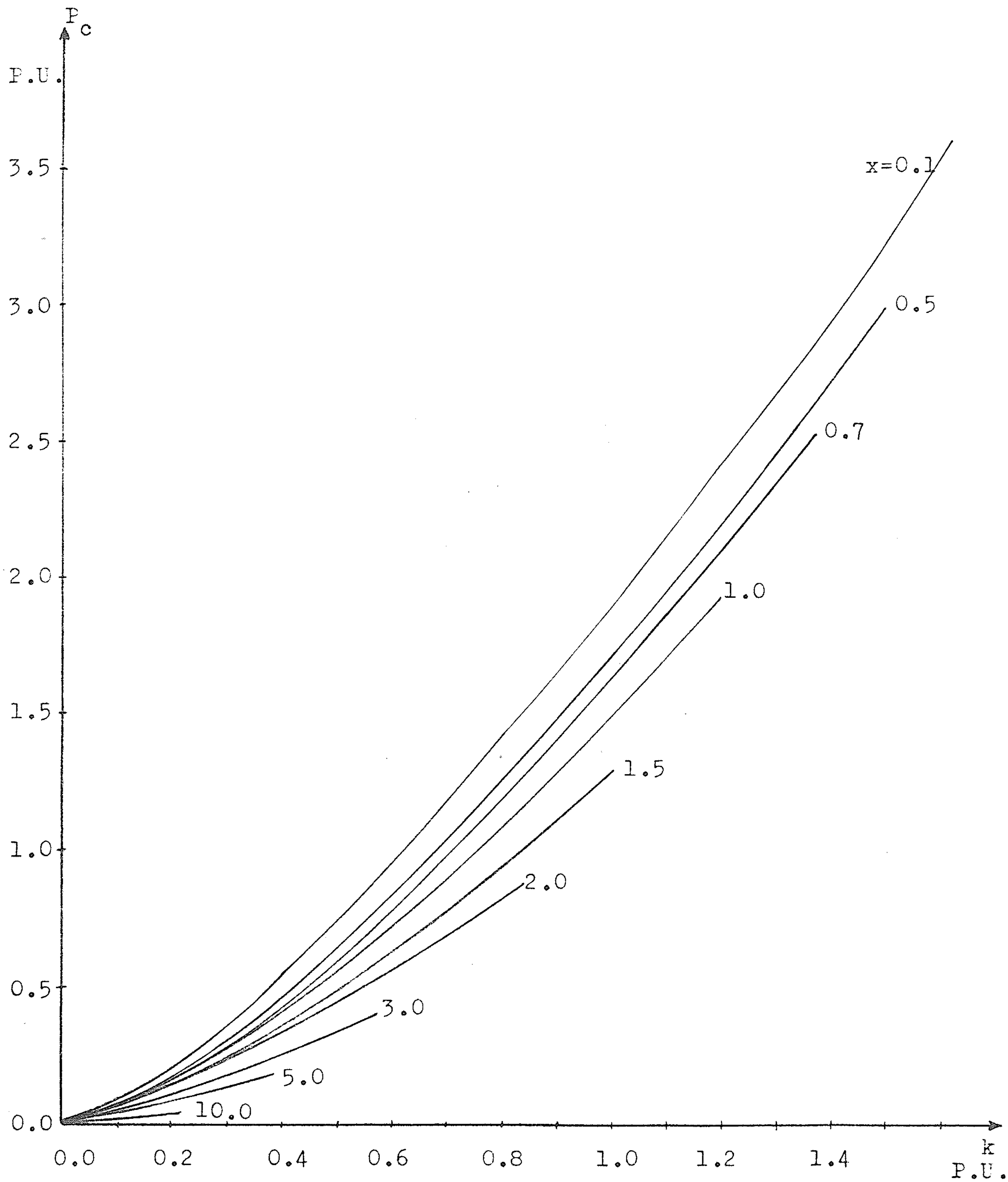

Fig. 21 - Copper Loss .

3.7 Magnetizing Voltage

Let $v_1(t)$ and $v_2(t)$ be the voltages across L_1 and $\overline{L}$, respectively, and $v(t) = v_1(t) + v_2(t)$ (see Fig. 10). Then,

$$v(\omega t) = k - \sqrt{2}\sin\omega t - i(\omega t) \quad \text{p.u.} \tag{30}$$

where, $i(\omega t)$ is given by (14a-f) for $k < \frac{\sqrt{2}}{\sqrt{1+x^2}}$, and by (16) for $k \geq \frac{\sqrt{2}}{\sqrt{1+x^2}}$. And,

$$V_{RMS}^2 = \frac{1}{2\pi}\int_{-\pi}^{\pi} [v(\omega t)]^2\, d(\omega t) = \frac{1}{2\pi}\int_{-\pi}^{\pi} (k - \sqrt{2}\sin\omega t - i(\omega t))^2\, d(\omega t) \tag{31}$$

Performing the integral, results in:

$$V_{RMS} = \sqrt{1 + k^2 - I_{RMS}^2} \quad \text{p.u.} \tag{32}$$

where, I_{RMS} is given by equations (26a) and (26b).

For $k \geq k_c$, equation (32) can be reduced to

$$V_{RMS} = \frac{x}{\sqrt{1+x^2}} \quad \text{p.u.} \tag{33}$$

V_{RMS} is plotted versus k and for different x, in Fig. 22.

The magnetizing voltage $v_2(t)$ is calculated as follows:

$$v_2(t) = \begin{cases} k - \sqrt{2}\sin\omega t & \alpha < \omega t < 2\pi - \theta \\ \frac{x_2}{x}\, v(t) & -\theta < \omega t < \alpha \end{cases} \qquad k < k_c \tag{34}$$

$$v_2(t) = \frac{x_2}{x}\, v(t) \qquad k \geq k_c \tag{35}$$

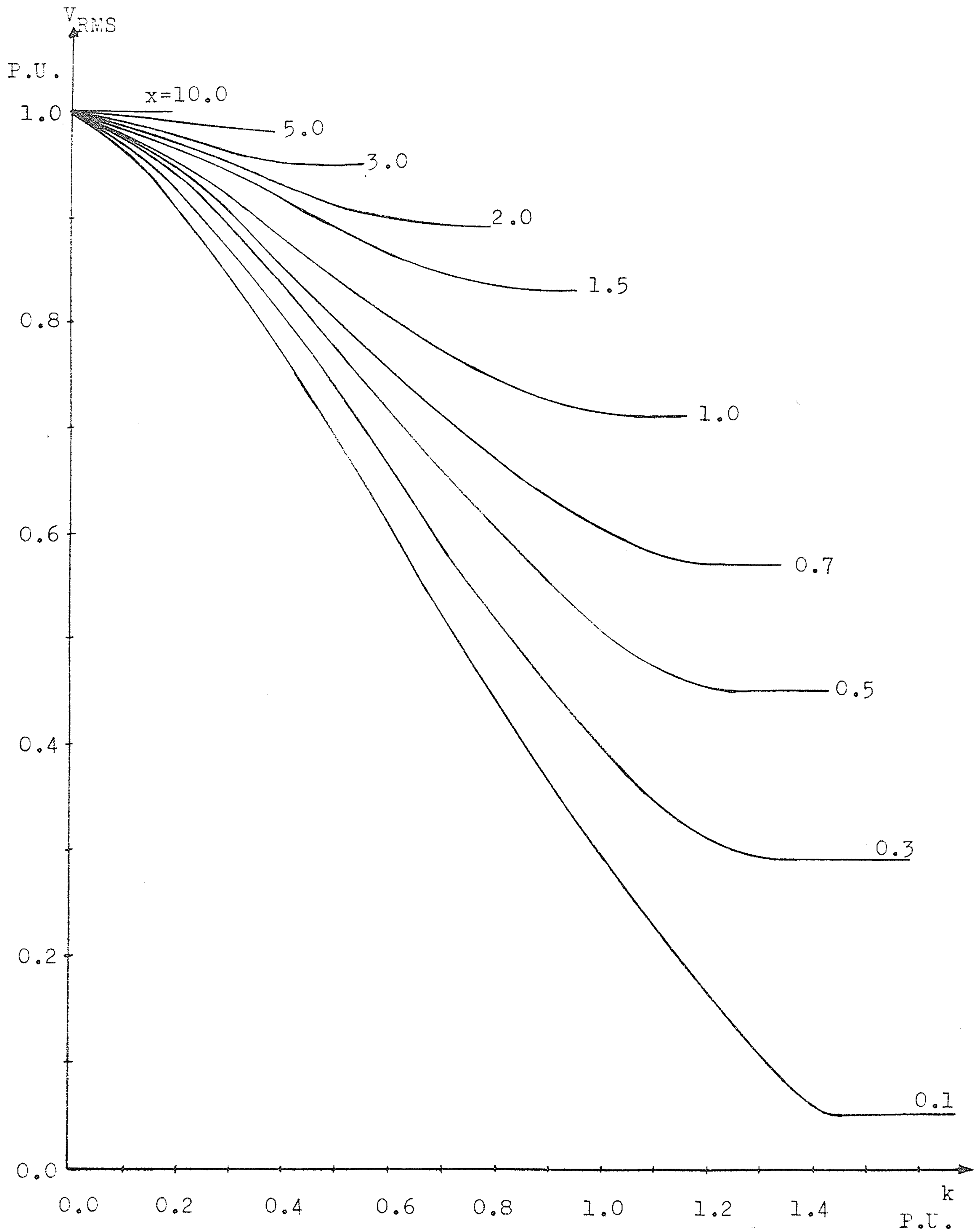

Fig. 22-Effective Voltage Of Non-Resistive Part.

$$V_{2RMS}^2 = \begin{cases} \dfrac{1}{2\pi} \displaystyle\int_{-\theta}^{2\pi-\theta} [v_2(\omega t)]^2 \, d(\omega t) & k < k_c \\ & \qquad\ldots(36) \\ \left(\dfrac{x_2}{x} \right)^2 V_{RMS}^2 & k \geq k_c \end{cases}$$

Performing the integral, results in:

$$V_{2RMS}^2 = \left(\frac{x_2}{x} \right)^2 (1 + k^2 - I_{RMS}^2) + \left[1 - \left(\frac{x_2}{x} \right)^2 \right] \left[\frac{1 - k^2}{2\pi} (2\pi - (\alpha+\theta)) + \frac{\sin 2\theta + \sin 2\alpha}{4\pi} \right] \quad k < k_c \quad (37)$$

$$V_{2RMS}^2 = \frac{x_2^2}{1 + x^2} \quad k \geq k_c \quad (38)$$

where, I_{RMS} is given by equations (26a) and (26b).

V_{2RMS}^2 can be expressed as follows:

$$V_{2RMS}^2 = \left(\frac{x_2}{x} \right)^2 D_1 + D_2 \quad (39)$$

where,

$$D_1 = \begin{cases} 2k^2 - I_{RMS}^2 + \dfrac{1 - k^2}{2\pi} (\theta + \alpha) - \dfrac{\sin 2\theta + \sin 2\alpha}{4\pi} & k < k_c \\ \dfrac{x^2}{1 + x^2} = V_{RMS}^2 & k \geq k_c \qquad \ldots(40) \end{cases}$$

$$D_2 = \begin{cases} \dfrac{(1 - k^2)}{2\pi} (2\pi - (\alpha + \theta)) + \dfrac{\sin 2\theta + \sin 2\alpha}{4\pi} & k < k_c \\ 0 & k \geq k_c \qquad \ldots(41) \end{cases}$$

D_1 and D_2 are plotted in Fig. 23 and 24. Equation (39), together with D_1 and D_2, gives the magnetizing voltage.

3.8 Iron losses

The total iron loss is the average real power in R_m. R_m has been ignored in calculations so far $(R_m = \infty)$. Nevertheless R_m is not infinity and can be found for any transformer, as was mentioned in section 2.1. Thus the iron losses can be expressed as

$$P_I = \frac{(\text{RMS magnetizing voltage})^2}{R_m} \tag{42}$$

RMS value of the magnetizing voltage will not differ from V_{2RMS} (calculated in section 3.7) materially, since in practice R_m turns out to be quite large. Thus

$$P_I = \frac{V_{2RMS}^2}{R_m} \quad \text{p.u.} \tag{43}$$

Substituting for V_{2RMS}^2 from equation (39)

$$P_I = \frac{1}{R_m}\left(\left(\frac{x_2}{x}\right)^2 D_1 + D_2\right) \tag{44}$$

Thus iron loss can be easily calculated by equation (44), along with Fig. 23 and 24, for any value of k.

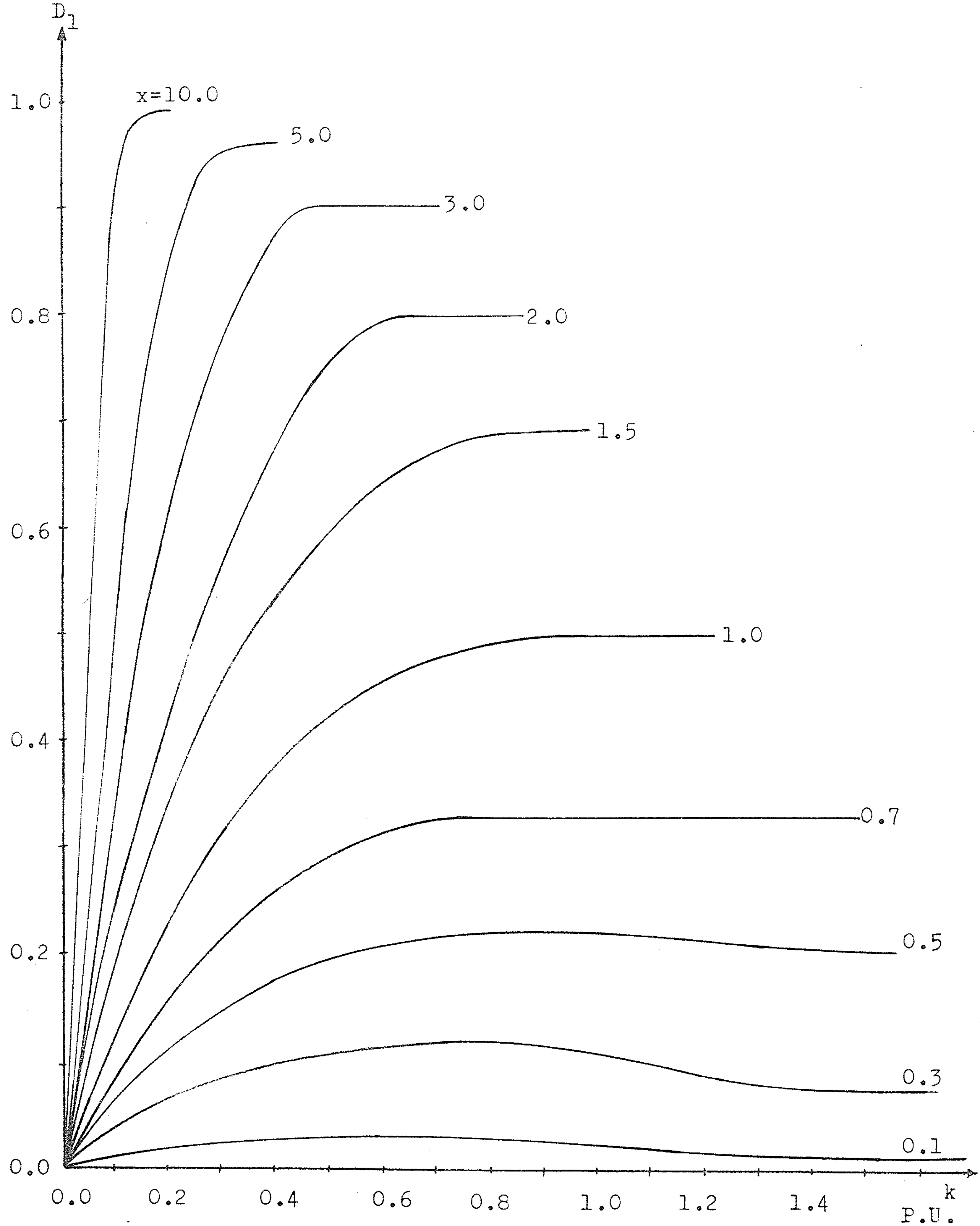

Fig. 23- Auxiliary Function D_1 .

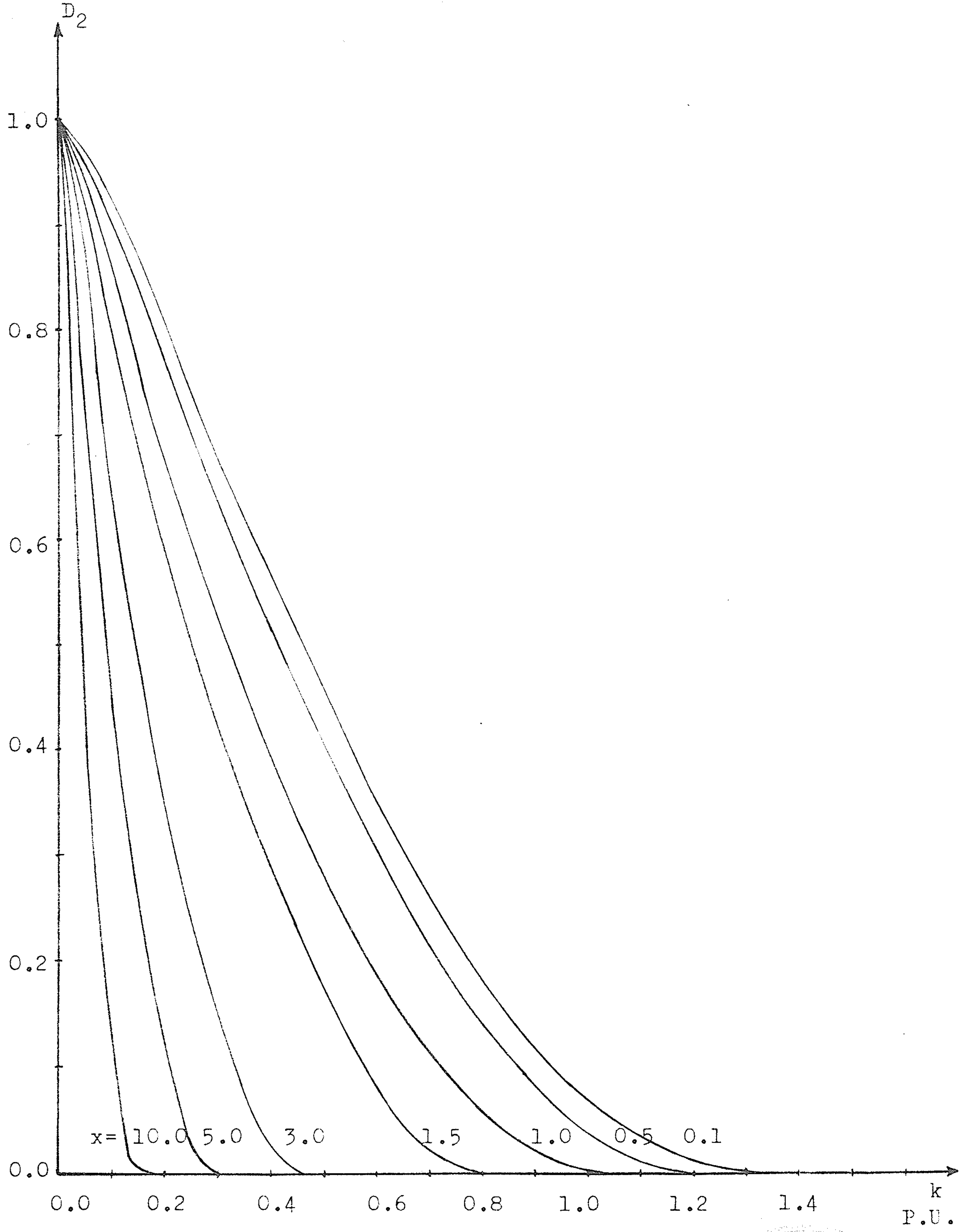

Fig. 24- Auxiliary Function D_2 .

3.9 Var Demands

The Var demands Q can be interpreted as the apparent power of the non-resistive part of the impedance in the circuit (L_1 and $\bar{L}$). The reason for this interpretation is that no energy is lost in L_1 and $\bar{L}$, as is shown below.

$$\text{Energy in non-resistive part over one period} = \frac{1}{\omega} \int_{\omega t=-\theta}^{\omega t=2\pi-\theta} v(\omega t) i(\omega t) d(\omega t)$$

$$= \frac{1}{\omega} \int_{\omega t=-\theta}^{\omega t=\alpha} \left(x \frac{di(\omega t)}{d(\omega t)}\right) i(\omega t)\, d(\omega t)$$

$$= \frac{x}{\omega} \int_{i=0}^{i=0} i\, di = 0 \tag{45}$$

Thus

$$Q = V_{RMS}\, I_{RMS} \quad \text{p.u.} \tag{46}$$

where V_{RMS} and I_{RMS} are given by equations (34) and (26a & b), respectively.

Q is plotted versus k and for different x, in Fig. 25.

According to the above, the Var demand of the magnetizing branch ($\bar{L}$) is

$$Q_2 = V_{2RMS}\, I_{RMS}$$

$$= \left[\left(\frac{x_2}{x}\right)^2 D_1 + D_2 \right] I_{RMS}$$

$$= \left(\frac{x_2}{x}\right)^2 D_3 + D_4 \tag{47}$$

where,

$$D_3 = I_{RMS}\, D_1 \tag{48a}$$

$$D_4 = I_{RMS}\, D_2 \tag{48b}$$

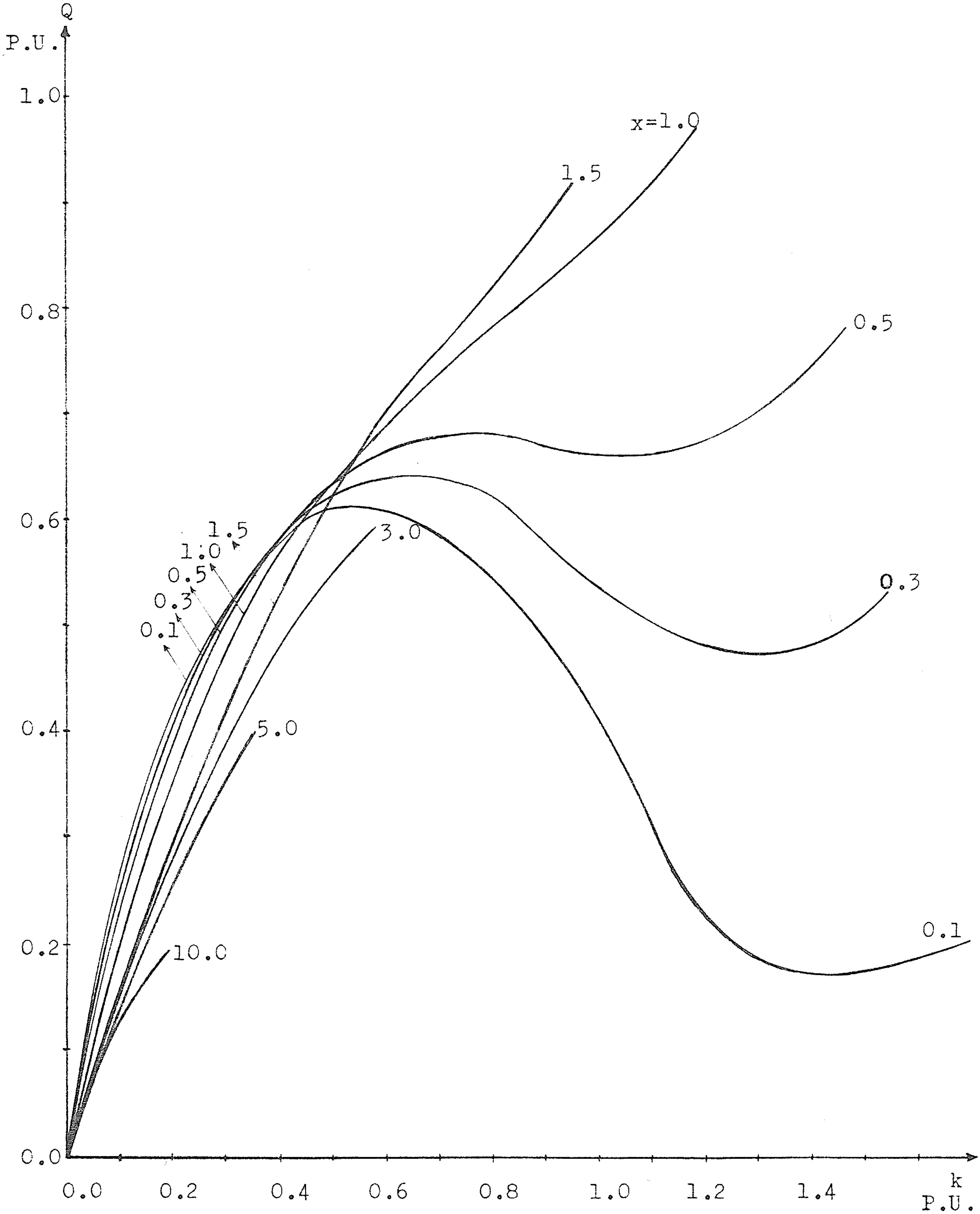

Fig. 25- Var Demands .

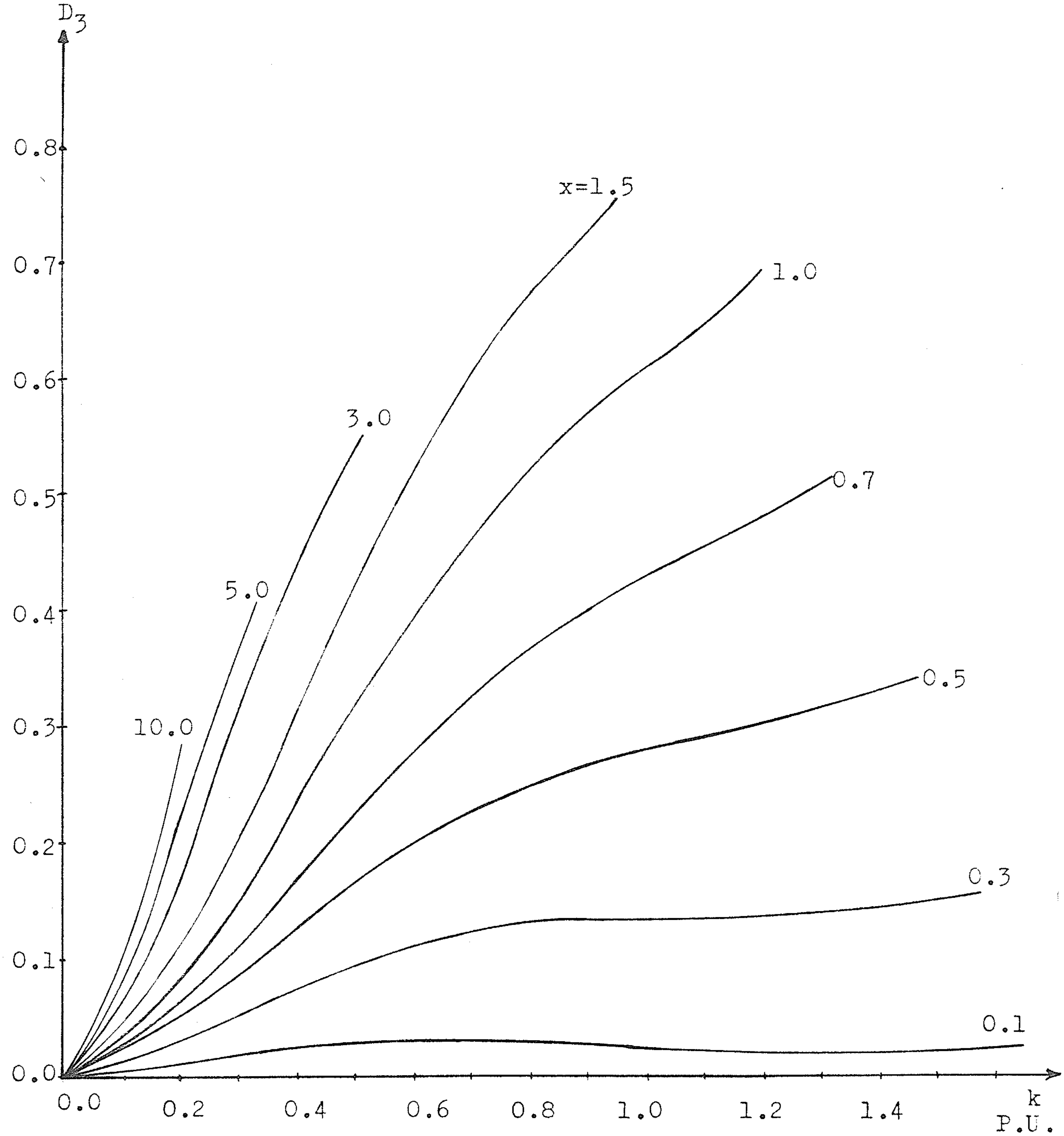

Fig. 26- Auxiliary Function D_3 .

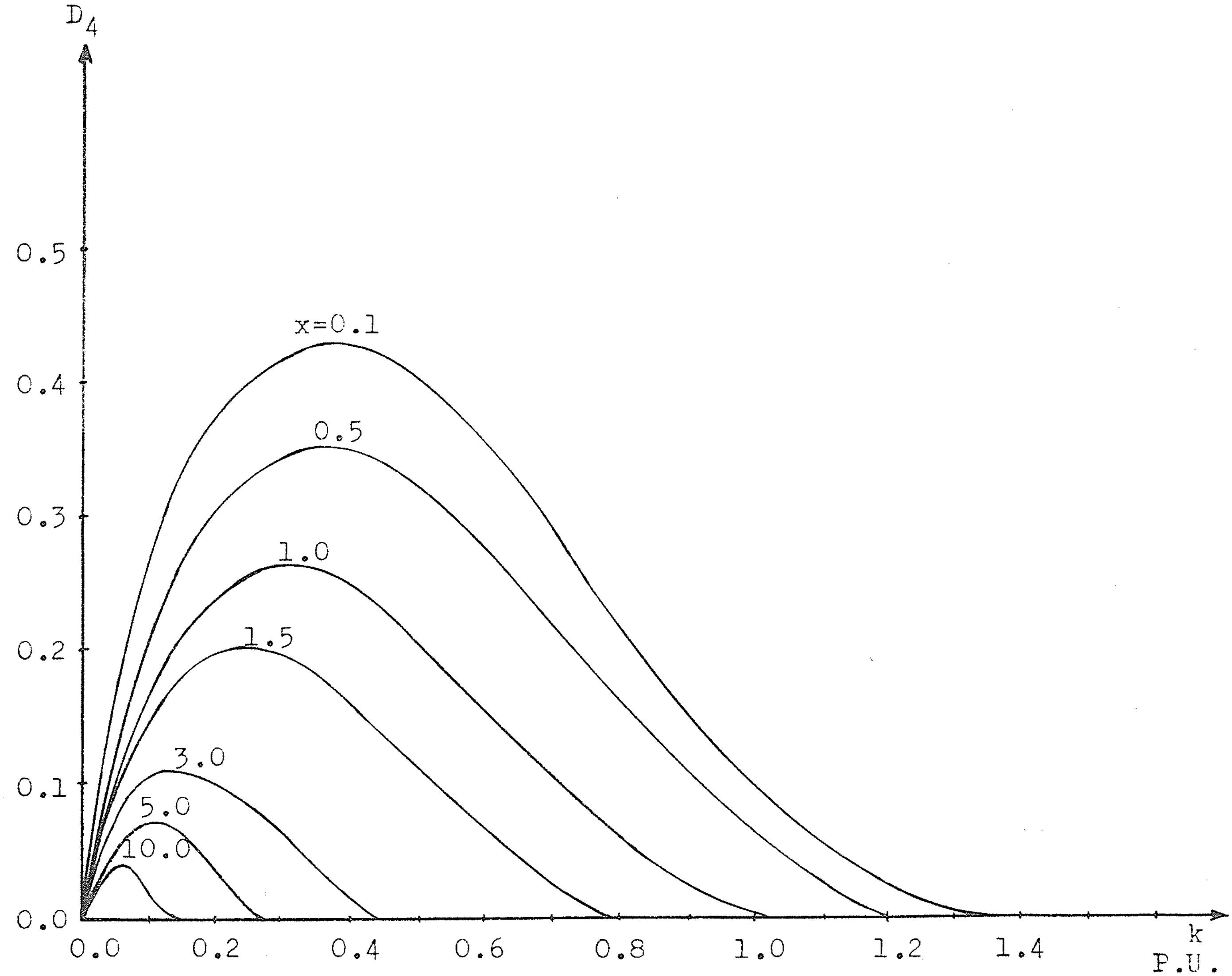

Fig. 27- Auxiliary Function D_4 .

and, D_1, D_2 and I_{RMS} are given by equations (40), (41) and (26a & b), respectively.

D_3 and D_4 are plotted in Fig. 26 and 27.

Q_2 can be calculated by equation (47), along with Fig. 26 and 27, for any value of k .

3.10 Apparent Power

The total apparent power S is calculated as follows

$$S = \left(\frac{1}{2\pi} \int_{-\pi}^{\pi} [k - \sqrt{2}\sin\omega t]^2 \, d(\omega t) \right)^{1/2} \left(\frac{1}{2\pi} \int_{-\pi}^{\pi} [i(\omega t)]^2 \, d(\omega t) \right)^{1/2}$$

$$= (1 + k^2)^{1/2} I_{RMS} \qquad \text{p.u.} \tag{49}$$

where I_{RMS} is given by equations (26a) and (26b).

It can easily be shown that

$$S^2 = P_c^2 + Q^2 \tag{50}$$

where, P_c and Q are defined by equations (31) and (46).

S is plotted versus k and for different x , in Fig. 28.

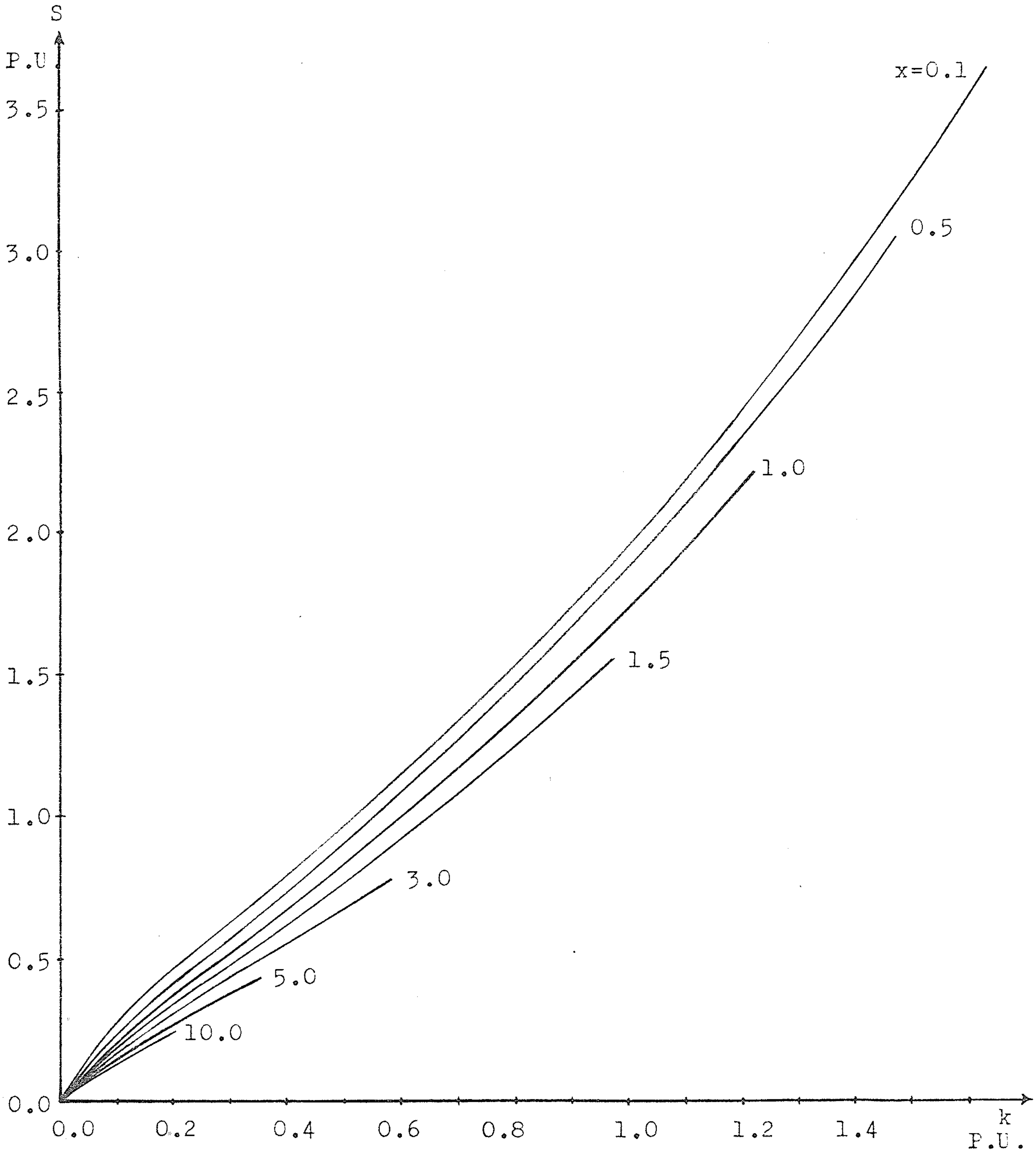

Fig. 28- Apparent Power .

3.11 Active Apparent Power, Reactive Apparent Power and Distortion Power

According to the definitions of Reference [11] , the total apparent power S may be resolved into three analytical components defined as the active apparent power S_R , the true reactive apparent power S_x and the distortion power S_D , where,

$$S_R^2 = (1 + k^2)(k^2 + I_{R1}^2) \quad \text{p.u.} \tag{51}$$

$$S_x^2 = (1 + k^2)\, I_{x1}^2 \quad \text{p.u.} \tag{52}$$

$$\begin{aligned} S_D^2 &= (1 + k^2) \sum_{n=2}^{\infty} I_n^2 \\ &= (1 + k^2)(I_{RMS}^2 - I_1^2 - k^2) \quad \text{p.u.} \end{aligned} \tag{53}$$

where I_{R1}, I_{x1}, I_1, I_n and I_{RMS} are given by equations (19a & b), (20a & b), (21a & b), (24a & b) and (26a & b) , respectively.

In general (for non sinusoidal systems), $S_R \neq P_c$ and $S_x \neq Q$ and $S_D \neq 0$. S_R, S_x and S_D are plotted versus k and for different x , in Fig. 29, 30 and 31, respectively.

S_R , S_x and S_D sum to S as follows:

$$S^2 = S_R^2 + S_x^2 + S_D^2 \tag{54}$$

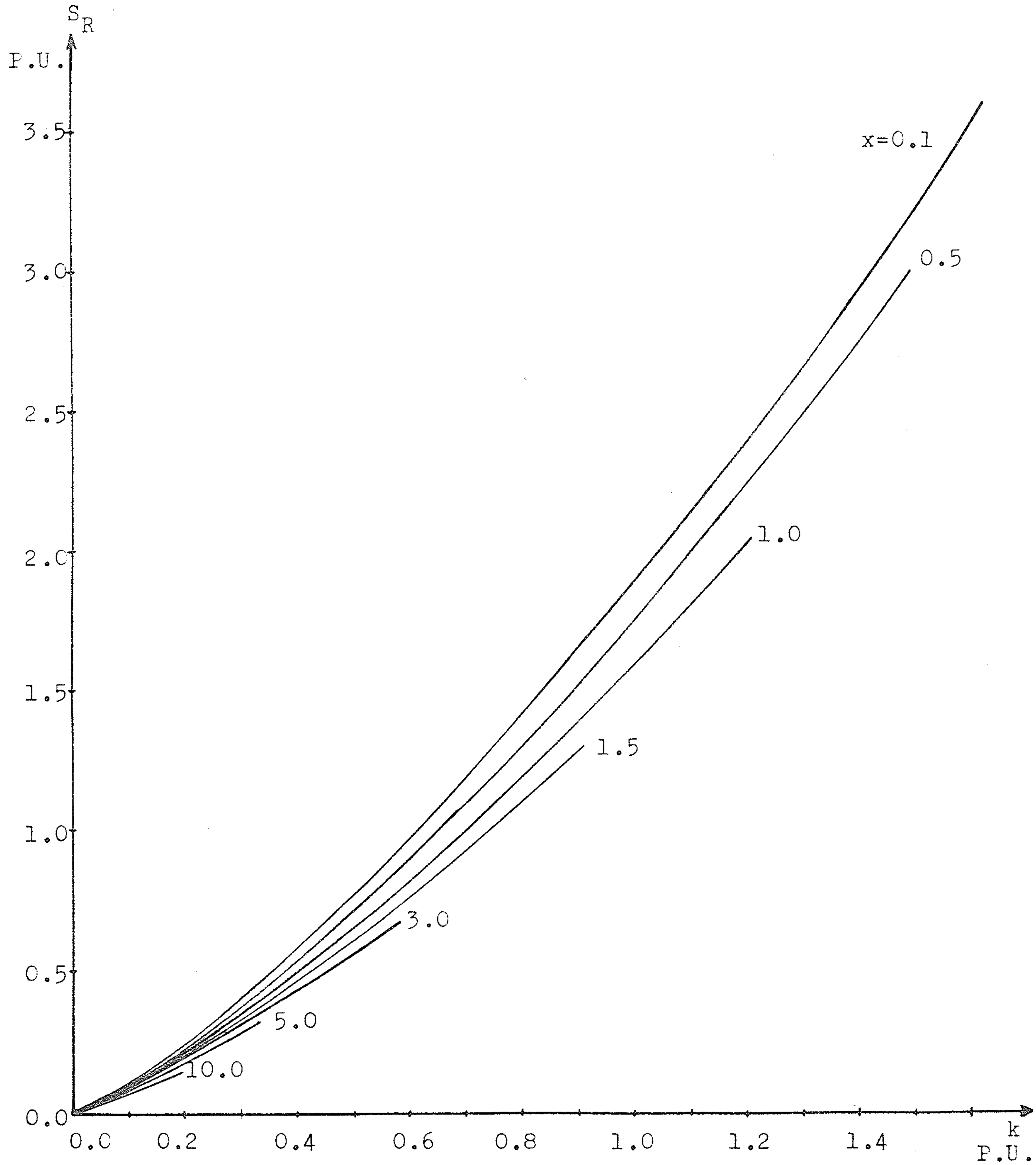

Fig. 29- Active Apparent Power .

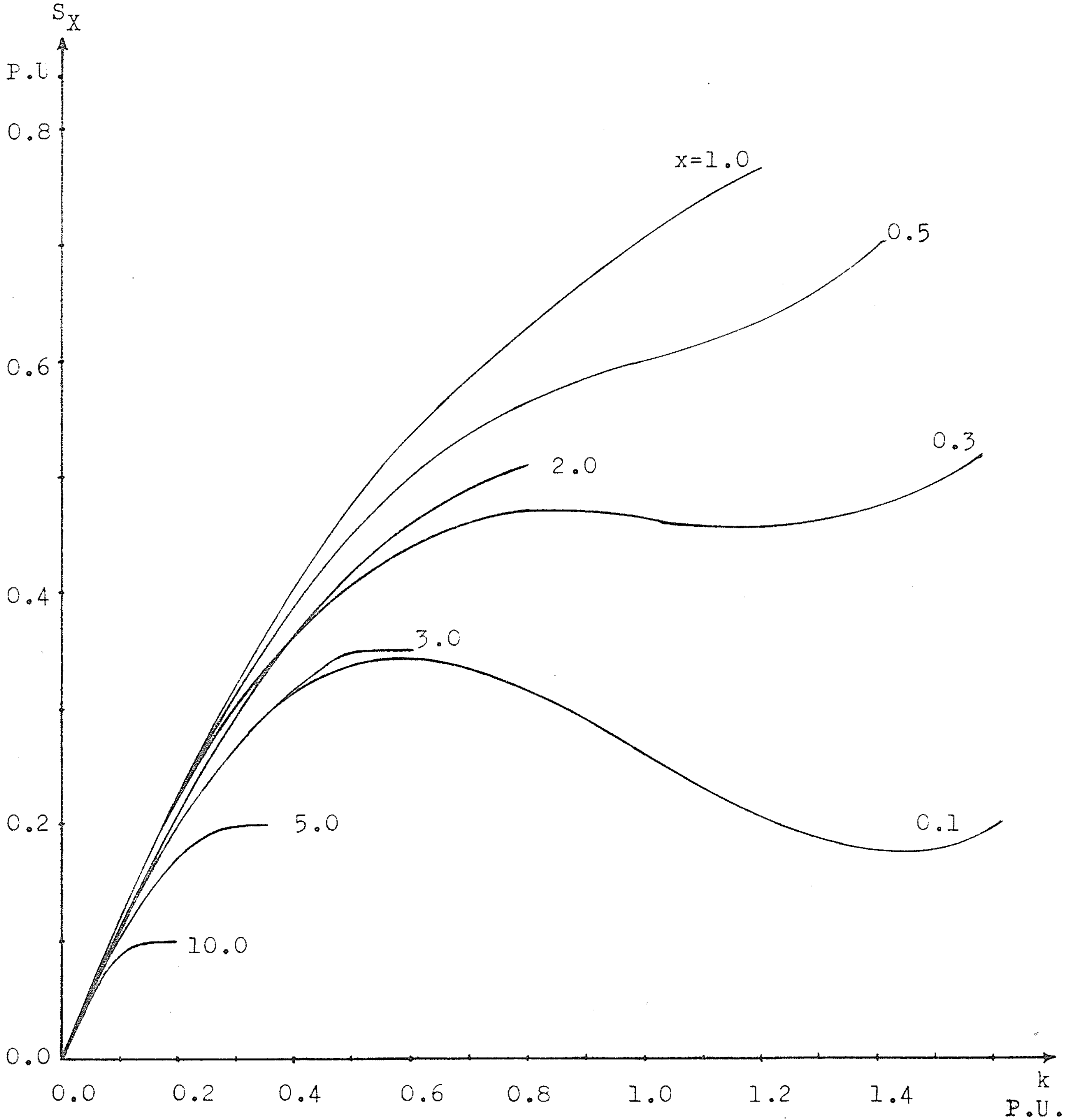

Fig. 30- Reactive Apparent Power .

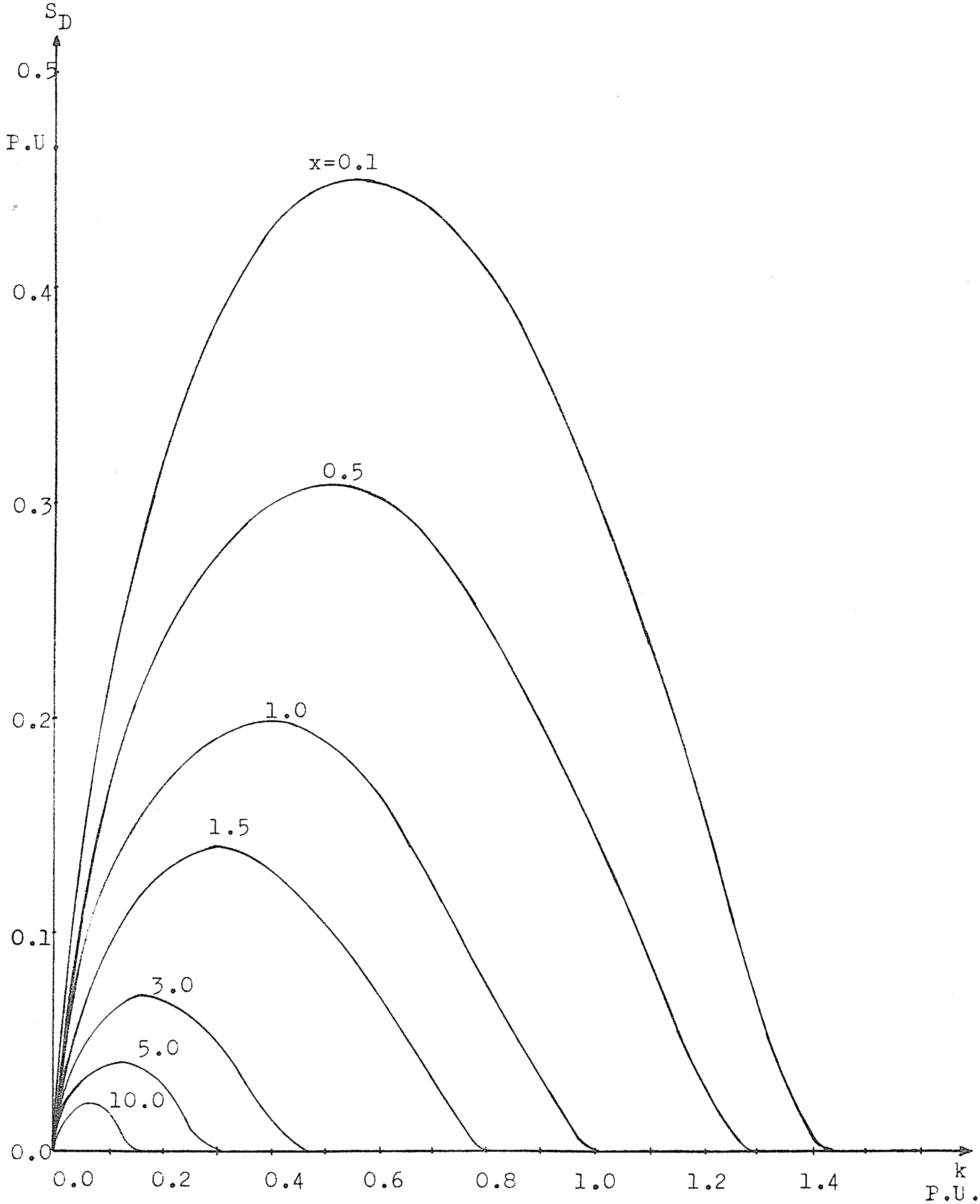

Fig. 31- Distortion Power .

3.12 Power Factor

In any circuit, linear or nonlinear, regardless of the waveform, the Power Factor is the factor by which the total apparent power must be multiplied to obtain the average real power [11] . Therefore

$$P.F. = \frac{P_c}{S} = \frac{I_{RMS}}{\sqrt{1+k^2}} \qquad (55)$$

where, I_{RMS} is given by equations (26a) and (26b).

If circuit compensation is sought, the maximum Power Factor is realized by compensation of S_x . S_x cannot be totally compensated by means of energy-storage devices, but can be reduced to a minimum value. However, a Power Factor of unity cannot be realized at all.

P.F. defined by equation (55) is plotted versus k and for different x , in Fig. 32.

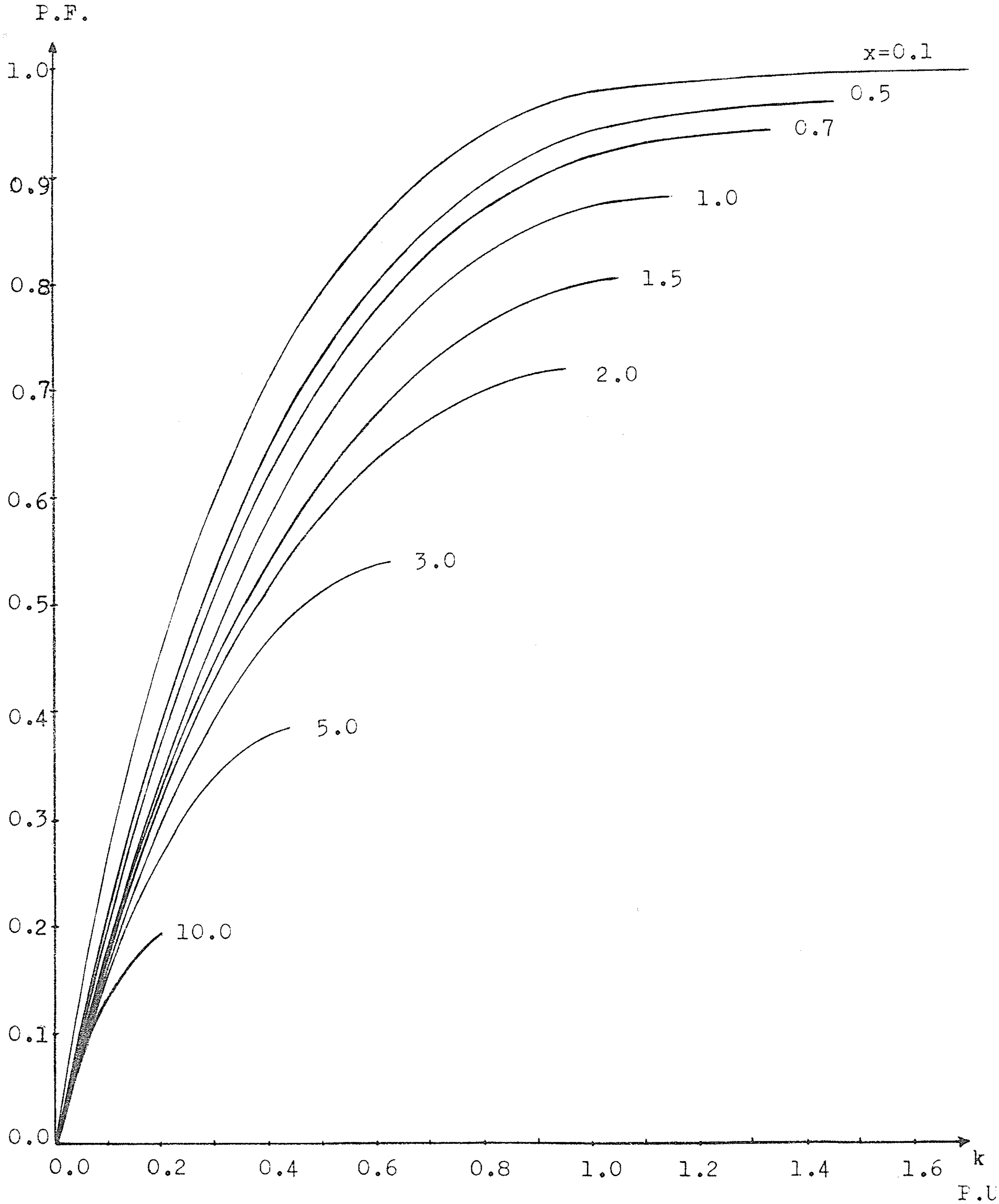

Fig. 32- Power Factor .

CHAPTER 4

DISCUSSION OF THE RESULTS

4.1 Validity of the Results

Due to approximations made in Chapter 2, there may appear some errors in the results, although insignificant. The major source of error is the idealized magnetizing curve. To show the effects of this idealization, the actual and simulated currents are plotted in Fig. 33 for a slight saturation case, and in Fig. 34 for a deep saturation case, by mapping the flux $\phi(t)$ through the actual and idealized magnetizing curves. The effect of neglecting R_m is the lack of the small current indicated in unsaturated region for the actual current. This small current, as compared to the RMS value (or maximum value) of the exciting current, is relatively lower for the deep saturation case than for the slight one. However, this current is so small that it will not affect the results considerably. The highest error arises at the points corresponding to the knee of the magnetizing curve which is badly simulated. As we can see, this error is relatively lower for the deep saturation case than the slight one. In other words, altogether, the error decreases as the case becomes more practical, and is insignificant for severe geomagnetic storms (not very small values of k). All the quantities calculated in Chapter 3 (Fig. 13 through 32) depend on the exciting current and thus are valid except for very small values of k $(k \ll k_c)$.

The assumption of k as constant does not produce any significant error as long as the period under consideration is short enough compared to the period of the geomagnetic fluctuations and is

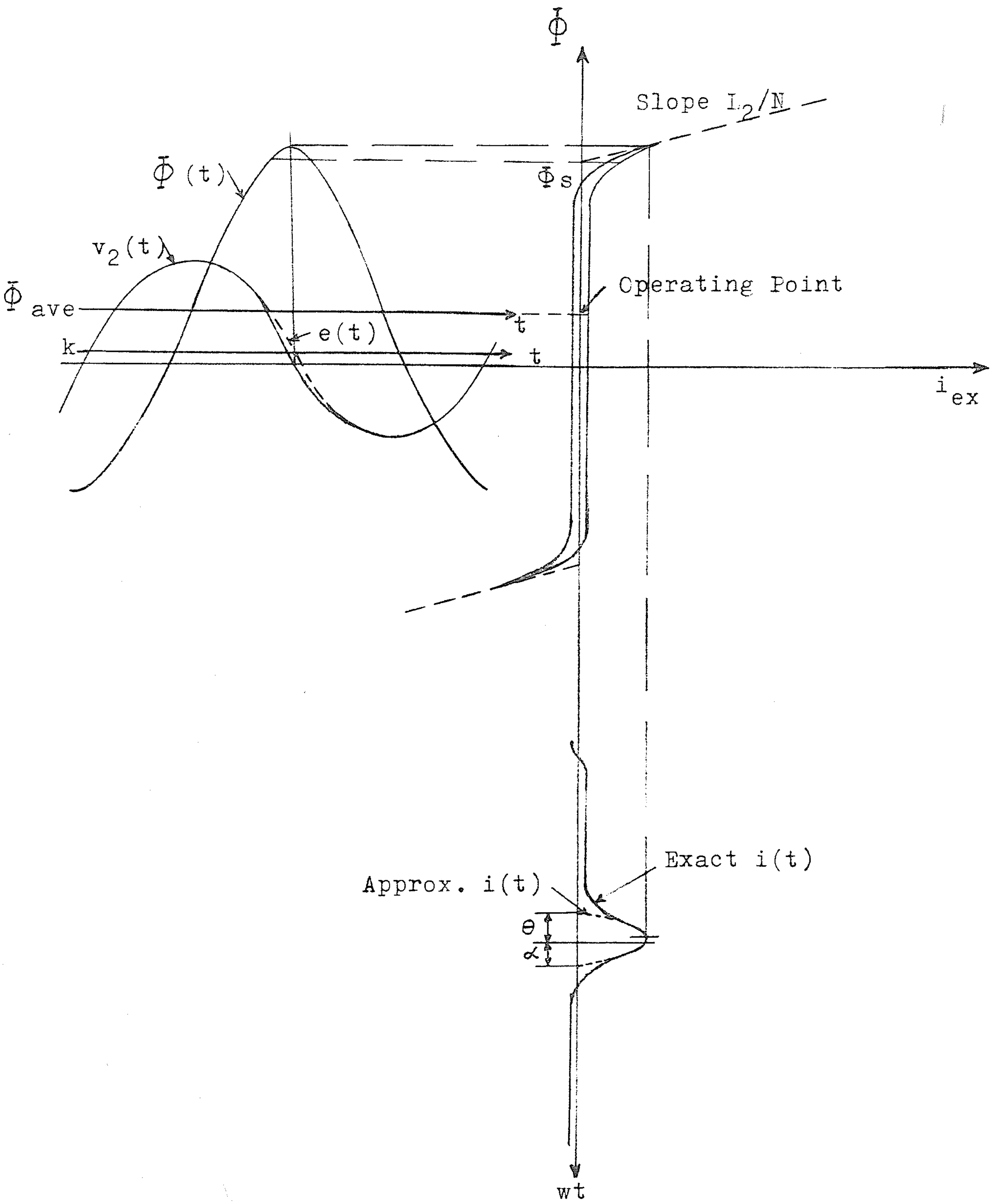

Fig.33- The Effect Of Idealization For Slight Saturation.

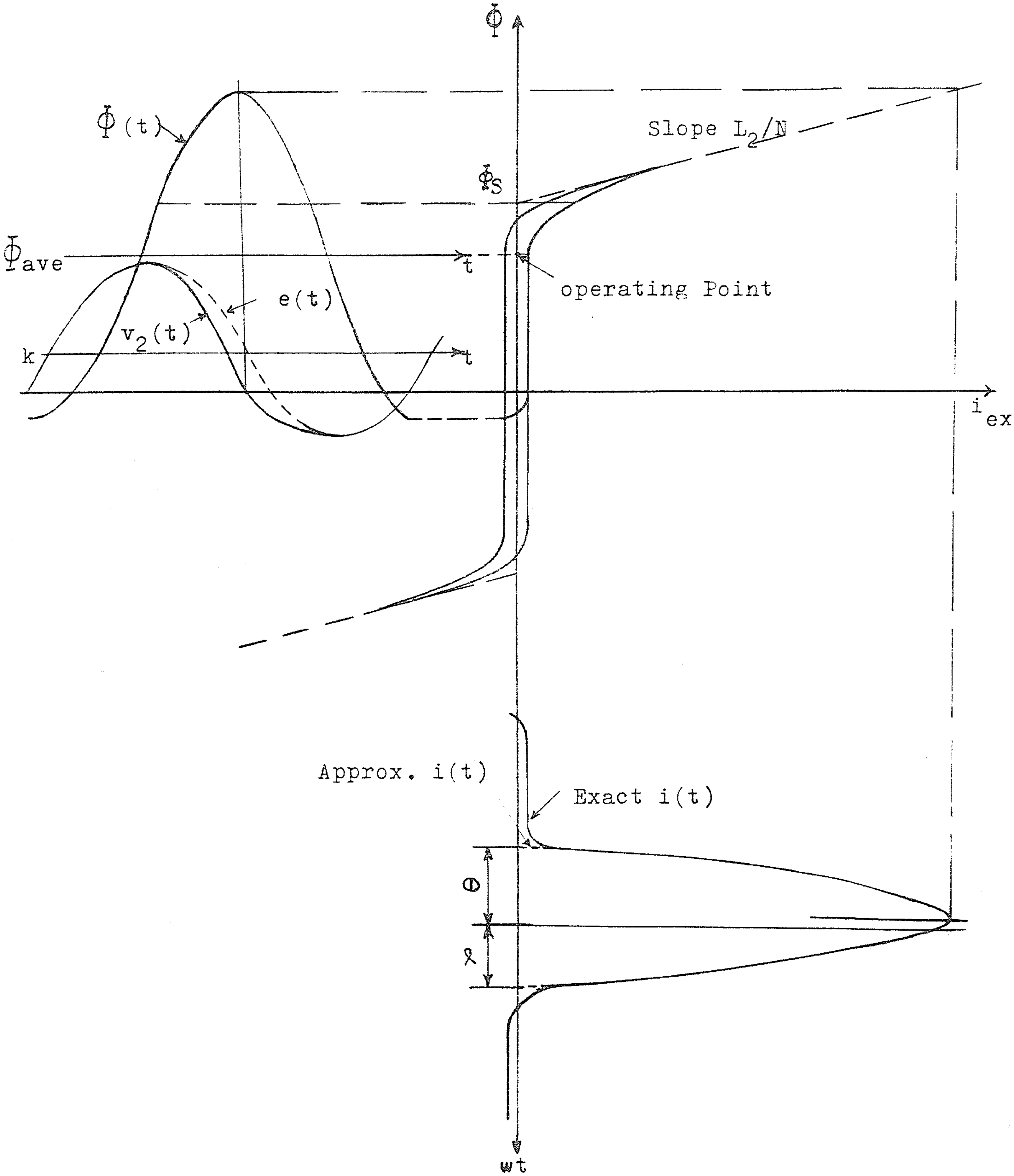

Fig.34- The Effect Of Idealization For Deep Saturation.

long enough compared to the time needed for reaching the steady state. After any significant change in k, it must be reevaluated.

4.2 Comments on the Results

The harmonics have been computed only upto 5th one. Higher order harmonics have very small magnitudes compared with fundamental. To show their effectiveness, the RMS current was computed using only upto 5th harmonic including fundamental. The result showed insignificant difference from the exact value of I_{RMS} shown in Fig. 20. However, any higher order harmonic may easily be computed using equations (22), (23) and (24).

The copper loss shown in Fig. 21 is in fact the increased (above the normal operating condition) copper loss due to GIC; since for $k = 0$, $i = 0$ has been assumed. Both ac and dc sources contribute to this increased loss. The contribution of dc source is k^2 p.u. or $\frac{3k^2}{R}$ watts.

The magnetizing voltage, being calculated by means of equation (39) and auxiliary functions D_1 and D_2, is always somewhat lower than V_{RMS} shown in Fig. 22 (they will be the same if the leakage reactance x_1 is neglected), and higher than $(x_2/x)V_{RMS}$ since $D_2 \neq 0$. This means that the two reactances do not simply act as voltage divider and the magnetizing voltage is closer to V_{RMS} than it seems to be. Only after complete saturation $V_{2RMS} = x_2/xV_{RMS}$.

The iron loss, calculated by means of equation (44) is always less than that of normal operating conditions ($\frac{1}{Rm}$ p.u.) , since V_{2RMS} is always less than 1 p.u. .

It can easily be shown that for $k \geq \sqrt{\frac{1}{Rm}}$ (which is usually the case),

$$P_c + P_I > \frac{1}{R_m} \quad \text{p.u.} \tag{56}$$

which indicates increase in total losses due to GIC.

The Var demands Q is also the increased Var demands due to GIC, since for $k = 0$, $Q = 0$. Q_2 is always less than Q and larger than $x_2/x\ Q$, and $Q_2 = x_2/x\ Q$ only after complete saturation. S, S_R, S_x and S_D are also assumed zero for no GIC.

All the graphs in Chapter 3 have been plotted for different values of x between 0.1 and 10. For very large transformers, x may turn out to be larger than 10. For such a particular case, we can either plot the graphs for larger values of x with larger scale or compute the quantities directly from their expressions. The sample calculation is shown for Dorsey 230-500 kV auto-transformer (see appendix), where, $x = 28.57$ p.u. .

CHAPTER 5

APPLICATION OF THE RESULTS IN DETERMINATION OF OTHER DISTURBANCES IN POWER SYSTEMS CAUSED BY GIC

GIC's may affect power systems in different respects, mostly resulting from the half-cycle saturation of the transformer studied in this thesis. The increased real losses and increased Var demands can cause a voltage drop at the ~~load~~ and a change in real power flow in the system. To study these effects the behaviour of the transformer under GIC must be entered in the model developed for the load flow studies in a proper manner. One of the usual techniques, which is employed in reference [5] , is to represent the transformer with its leakage reactance (as usual), and to assign the increased Var demands to the transformer bus, for example half of it to either side. The real losses can be included as well.

To extinguish the secondary arc current during a single pole switching, shunt reactors are connected to the system to compensate for the fundamental frequency electrostatic coupling. These reactors can be affected by GIC similar to transformers. The half-cycle saturation of these reactors as well as transformers may cause higher harmonic magnitudes in the secondary arc current resulting in additional time to extinguish the arc [6] .

Another probable disturbance caused by GIC is relay operation problem which can be due to C.T. half-cycle saturation [4] . The dc component of the exciting current of the power transformer, passing through the winding of the C.T. in the line, times the series resistance of the C.T. winding serves as K . There may be several other disturbances in the system caused by GIC [5,6] which can be studied using the results of this thesis. These results altogether serve as a means to determine whether or not the mitigation of GIC is necessary. In fact mitigation of GIC is possible and several neutral devices have been realized so far [4, 12] .

At distribution level, various systems of rectifiers or symmetrical voltage peak limiters can produce a direct current in the system [13] affecting the involved transformers similar to GIC.

CHAPTER 6

CONCLUSIONS

This study allows to quantitatively evaluate the effects of GIC on transformers with a good approximation and for a wide range of the GIC. The results also reveal that:

1. GIC causes half-cycle saturation in power transformers. The degree of this saturation depends on the severity of the geomagnetic storm, as well as the ratio $\omega L/R$. For a given GIC, it increases with increasing $\omega L/R$.
2. The steady-state magnetizing current of the transformer under GIC is unidirectional (similar to inrush current) and its average is equal to the amplitude of the effective GIC flowing in the core.
3. The operating point on the magnetizing curve does not correspond directly to the amplitude of the GIC. It corresponds to the average flux which will establish itself in the core. The current corresponding to this point on the actual saturation curve is much less than GIC.
4. The RMS value of the magnetizing current of the transformer under GIC is many times greater than the normal one (with no GIC).
5. The steady-state magnetizing current of the transformer under GIC contains even as well as odd harmonics, with the magnitudes of the lower order harmonics intolerably high. Almost always the second harmonic has the highest

magnitude. Harmonics higher than 5th have negligible magnitudes so far as RMS current is concerned.

6. Due to GIC, copper loss of the transformer is increased. However, for Dorsey transformer it doesn't seem to be any problem.

7. Due to GIC, iron loss of the transformer is slightly decreased.

8. Altogether, due to GIC, the total real loss is increased.

9. Due to GIC, the voltage at secondary terminals is highly distorted. Its RMS value is somewhat decreased but is higher than the value obtained by voltage dividing across x_1 and x_2 .

10. The Var demand of the transformer under GIC is considerably increased.

REFERENCES

[1] V.D. Albertson and J.A. Baelen, "Electric and Magnetic Fields at the Earth's Surface Due to Auroral Currents," IEEE Transactions on Power Apparatus and Systems, Vol. PAS-89, Np. 2, pp. 578-584, April 1970.

[2] V.D. Albertson, R.E. Clayton, J.M. Thorson, Jr., and S.C. Tripathy, "Solar-Induced Currents in Power Systems: Cause and Effects," IEEE Transactions on Power Apparatus and Systems, Vol. PAS-92, No. 2, pp. 471-477, March/April 1973.

[3] V.D. Albertson and J.M. Thorson, Jr., "Power System Disturbances During a K-8 Geomagnetic Storm: August 4, 1972," ibid., pp. 1025-1030, July/August 1974.

[4] V.D. Albertson, S.A. Miske, and J.M. Thorson, Jr., "The Effects of Geomagnetic Storms on Electrical Power Systems," IEEE Transactions on Power Apparatus and Systems, Vol. PAS-93, No. 4, pp. 1030-1044, July/August 1974.

[5] V.D. Albertson, J.G. Kappenman, N. Mohan and G.A. Skarbakka, "Load-Flow Studies in the Presence of Geomagnetically-Induced-Currents," being submitted for presentation at the 1979 IEEE Summer Meeting in Vancouver, Canada, F79 702-2.

[6] N. Mohan, J.G. Kappenman and V.D. Albertson, "Harmonics and Switching Transients in the Presence of Geomagnetically-Induced Currents," being submitted for presentation at the 1979 IEEE Summer Meeting in Vancouver, Canada, F79 694-1.

[7] J. Aubin and L. Bolduc, "Effects of Direct Current on Power Transformers," IEEE Canadian Communication and Power Conference

1976, Cat. No. 76 CH1126-2 Reg. 7, p. 315.

[8] L.F. Blume, G. Camilli, S.B. Farnham and H.A. Peterson, "Transformer Magnetizing Inrush Currents and Influence on System Operation," AIEE Transactions, Vol. 63, 1944, pp. 366-374.

[9] W.K. Sonnemann, C.L. Wagner and G.D. Rockefeller, "Magnetizing Inrush Phenomena in Transformer Banks," AIEE Transactions, Vol. 77, pp. 884-892, October 1958.

[10] Theodore R. Specht, "Transformer Inrush and Rectifier Transient Currents," IEEE Transactions, PAS-88, pp. 269-276, April 1969.

[11] W. Shepherd and P. Zakikhani, "Suggested Definition of Reactive Power for Nonsinusoidal Systems," Proceedings of the Institution of Electrical Engineers, Vol. 119, No. 9, pp. 1361-1362, September 1972.

[12] S.C. Tripathy, "Effects of Magnetic Storms on Electric Power Systems," Ph.D. Thesis, University of Minnesota, September 1970.

[13] "Direct Currents in the m.v. network," Electrical Review, p. 54, January 17, 1975.

APPENDIX

APPENDIX

The results are determined for Dorsey 230-500 kV auto-transformer with secondary and tertiary open-circuited.

$E = 230/\sqrt{3} = 132.8$ kV (rms)

Zsource $= 0.85 + j\,7.14$ ohm

$R_p = 0.0565$ ohm

$R = 0.0565 + 0.85 = 0.9065$ ohm

$R_m = 444000$ ohm

Leakage reactance of the 230 kV side turns out to be negative with small magnitude which is assumed nil. Thus: $x_1 = 7.14$ ohm

x_2 is calculated from magnetizing curve of the transformer (from 230 kV side) shown in Fig. (A-1), as follows:

$$X_2 = 2\pi 60 \, \frac{913-628}{5812-82} = 18.75 \text{ ohm}$$

$$x = \frac{x_1 + x_2}{R} = 28.57 \text{ p.u.}$$

Fig. (A-1) is based on the information obtained from Manitoba Hydro. The results are shown on the next few pages for different effective GIC's (by choosing different values for γ) , where,

$$(GIC)_{effective} = \frac{N_{com} I_{com} + N_{ser} I_{ser}}{N_{com} + N_{ser}} = 0.46\, I_{com} + 0.54\, I_{ser}$$

(see ref. [6])

and

I_{com} = The direct current in common winding.

I_{ser} = The direct current in series winding.

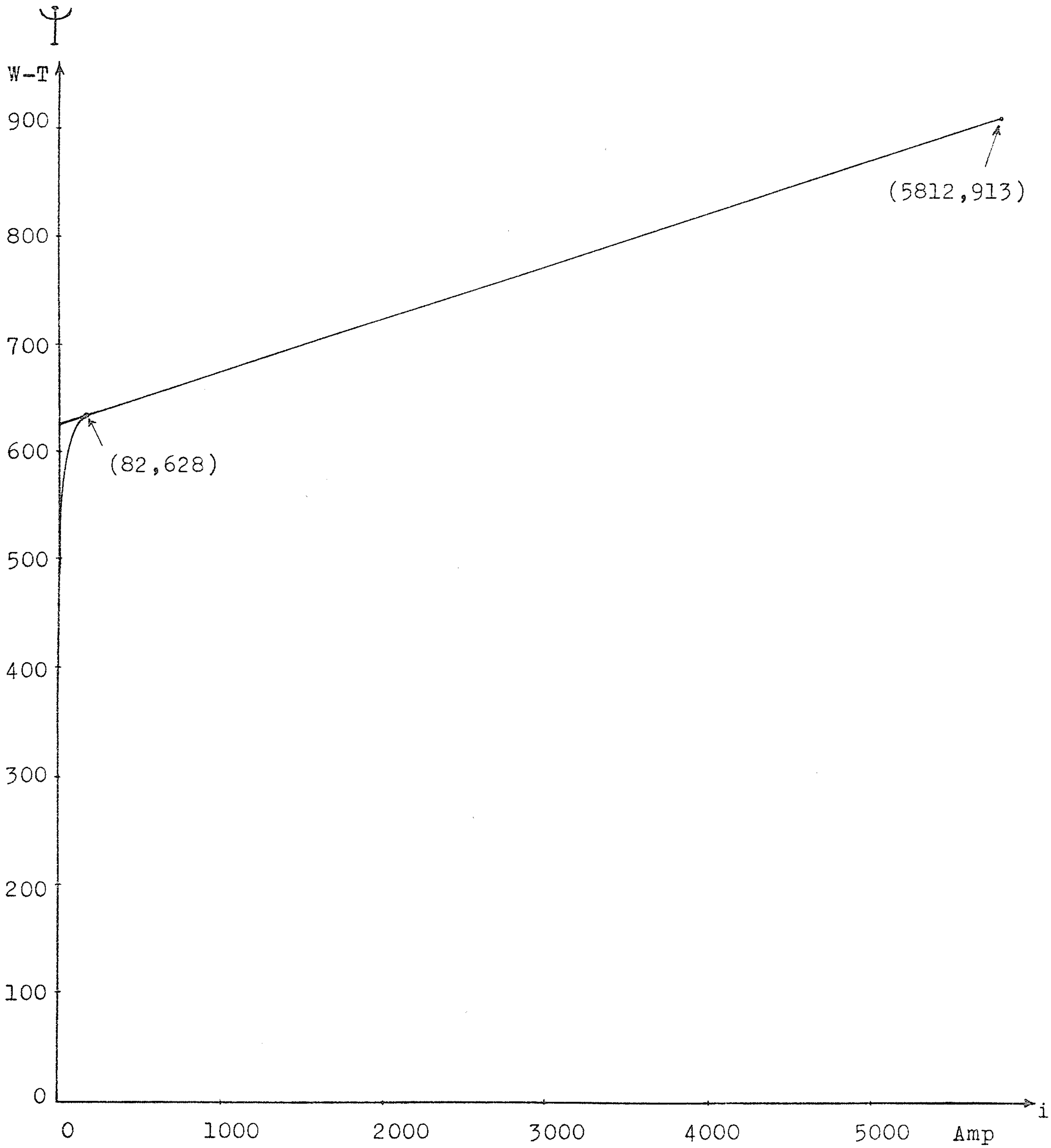

Fig.(A-1)- Dorsey Autotransformer's Magnetizing Curve.

x= 28.57 p.u.

(1) GAMA RAD.	(2) GIC AMP	(3) TETA DEG.	(4) ALPHA DEG.	(5) IR1 AMP	(6) IX1 AMP	(7) I1 AMP	(8) I2/I1	(9) I3/I1	(10) I4/I1	(11) I5/I1	(12) IRMS AMP	(13) IRMSF AMP
0.48	10.6	13.8	13.7	0.01	14.9	14.9	0.983	0.955	0.916	0.868	38.7	33.2
0.50	12.0	14.4	14.3	0.01	16.8	16.8	0.981	0.951	0.909	0.858	44.3	37.3
0.52	13.5	14.9	14.9	0.02	18.9	18.9	0.980	0.947	0.902	0.847	48.8	41.8
0.54	15.0	15.5	15.4	0.02	21.1	21.1	0.978	0.943	0.895	0.835	54.5	46.5
0.56	16.6	16.1	16.0	0.02	23.5	23.5	0.977	0.939	0.887	0.824	59.3	51.6
0.58	18.7	16.7	16.6	0.03	26.1	26.1	0.975	0.934	0.879	0.812	66.0	57.0
0.60	20.6	17.2	17.1	0.03	28.9	28.9	0.973	0.930	0.871	0.800	72.7	62.7
0.62	22.7	17.8	17.7	0.04	31.8	31.8	0.971	0.925	0.863	0.787	77.6	68.7
0.64	25.0	18.4	18.3	0.05	34.9	34.9	0.970	0.920	0.854	0.775	85.2	75.1
0.66	27.4	19.0	18.8	0.05	38.3	38.3	0.968	0.915	0.846	0.762	91.8	81.9
0.68	30.0	19.6	19.4	0.06	41.8	41.8	0.966	0.910	0.837	0.748	98.7	89.0
0.70	32.6	20.1	20.0	0.07	45.5	45.5	0.964	0.905	0.828	0.735	106.3	96.4
0.72	35.4	20.7	20.5	0.08	49.5	49.5	0.962	0.900	0.818	0.721	114.1	104.2
0.74	38.4	21.3	21.1	0.09	53.6	53.6	0.959	0.895	0.809	0.707	122.2	112.3
0.76	41.7	21.9	21.7	0.11	58.0	58.0	0.957	0.889	0.799	0.693	130.5	120.9
0.78	45.0	22.4	22.3	0.12	62.6	62.6	0.955	0.883	0.789	0.679	139.1	129.7
0.80	48.5	23.0	22.8	0.14	67.4	67.4	0.953	0.878	0.779	0.665	148.4	138.9
0.82	52.2	23.6	23.4	0.15	72.5	72.5	0.950	0.872	0.769	0.650	157.5	148.5
0.84	56.0	24.2	24.0	0.17	77.8	77.8	0.948	0.866	0.759	0.635	167.6	158.4
0.86	60.1	24.7	24.5	0.19	83.4	83.4	0.946	0.859	0.748	0.620	177.6	168.7
0.88	64.2	25.3	25.1	0.22	89.2	89.2	0.943	0.853	0.738	0.606	188.2	179.4
0.90	68.7	25.9	25.7	0.24	95.2	95.2	0.940	0.847	0.727	0.590	198.6	190.4
0.92	73.3	26.5	26.2	0.26	101.5	101.5	0.938	0.840	0.716	0.575	209.8	201.8
0.94	78.1	27.1	26.8	0.29	108.1	108.1	0.935	0.834	0.705	0.560	221.2	213.5
0.96	83.1	27.6	27.4	0.32	114.9	114.9	0.932	0.827	0.694	0.545	232.9	225.6
0.98	88.4	28.2	27.9	0.36	122.0	122.0	0.930	0.820	0.683	0.530	244.9	238.1
1.00	93.6	28.8	28.5	0.39	129.4	129.4	0.927	0.813	0.671	0.514	257.5	250.9
1.02	99.4	29.4	29.1	0.43	137.0	137.0	0.924	0.806	0.660	0.499	270.5	264.0
1.04	105.3	29.9	29.6	0.47	144.9	144.9	0.921	0.799	0.648	0.484	283.7	277.6
1.06	111.4	30.5	30.2	0.52	153.1	153.1	0.918	0.792	0.636	0.468	297.2	291.5
1.08	117.7	31.1	30.8	0.57	161.6	161.6	0.915	0.785	0.625	0.453	311.0	305.7
1.10	124.2	31.7	31.3	0.62	170.4	170.4	0.912	0.777	0.613	0.438	325.4	320.3
1.12	130.9	32.3	31.9	0.67	179.4	179.4	0.909	0.770	0.601	0.422	340.1	335.3
1.14	137.9	32.8	32.5	0.73	188.8	188.8	0.906	0.762	0.589	0.407	355.1	350.6
1.16	145.1	33.4	33.0	0.79	198.4	198.5	0.902	0.755	0.577	0.392	370.5	366.2
1.18	152.5	34.0	33.6	0.86	208.4	208.4	0.899	0.747	0.565	0.377	386.3	382.2
1.20	160.3	34.6	34.2	0.93	218.7	218.7	0.896	0.739	0.553	0.362	402.3	398.6
1.22	168.2	35.2	34.7	1.01	229.2	229.2	0.892	0.731	0.541	0.347	418.8	415.3
1.24	176.4	35.7	35.3	1.08	240.1	240.1	0.889	0.723	0.529	0.333	435.7	432.4
1.26	184.9	36.3	35.9	1.17	251.3	251.3	0.885	0.715	0.517	0.318	452.9	449.9
1.28	193.6	36.9	36.4	1.26	262.7	262.7	0.882	0.707	0.505	0.304	470.5	467.6
1.30	202.5	37.5	37.0	1.35	274.5	274.5	0.878	0.699	0.492	0.290	488.5	485.8
1.32	211.7	38.1	37.6	1.45	286.6	286.6	0.875	0.691	0.480	0.275	507.0	504.3
1.34	221.2	38.6	38.1	1.55	299.1	299.1	0.871	0.683	0.468	0.262	525.7	523.1
1.36	230.9	39.2	38.7	1.66	311.8	311.8	0.867	0.674	0.456	0.248	544.8	542.3
1.38	240.9	39.8	39.3	1.78	324.9	324.9	0.864	0.666	0.444	0.234	564.3	561.9
1.40	251.2	40.4	39.8	1.90	338.3	338.3	0.860	0.658	0.432	0.221	584.2	581.8

(1) GAMA RAD.	(2) GIC AMP	(14) V2RMS KV	(15) PC KW	(16) PI KW	(17) P(IN.) KW	(18) Q MVAR	(19) Q2 MVAR	(20) S MVA	(21) SR MW	(22) SX MVAR	(23) SD MVA	(24) P.F.
0.48	10.6	499.7	4.1	119.0	3.9	15.4	15.4	15.4	4.2	5.9	13.6	0.0003
0.50	12.0	499.6	5.3	119.0	5.1	17.6	17.6	17.6	4.8	6.7	15.6	0.0003
0.52	13.5	499.6	6.5	118.9	6.2	19.4	19.4	19.4	5.4	7.5	17.1	0.0003
0.54	15.0	499.5	8.1	118.9	7.8	21.7	21.7	21.7	6.0	8.4	19.1	0.0004
0.56	16.8	499.5	9.6	118.9	9.3	23.6	23.6	23.6	6.7	9.4	20.7	0.0004
0.58	18.7	499.4	11.9	118.9	11.5	26.3	26.2	26.3	7.4	10.4	23.0	0.0005
0.60	20.6	499.3	14.4	118.8	14.0	29.0	28.9	29.0	8.2	11.5	25.3	0.0005
0.62	22.7	499.3	16.4	118.8	16.0	30.9	30.8	30.9	9.0	12.7	26.7	0.0005
0.64	25.0	499.2	19.8	118.8	19.3	34.0	33.9	34.0	9.9	13.9	29.3	0.0006
0.66	27.4	499.1	22.9	118.7	22.5	36.6	36.5	36.6	10.9	15.2	31.4	0.0006
0.68	30.0	499.0	26.5	118.7	26.0	39.3	39.2	39.3	11.9	16.6	33.6	0.0007
0.70	32.6	498.9	30.7	118.6	30.2	42.4	42.2	42.4	13.0	18.1	36.0	0.0007
0.72	35.4	498.9	35.4	118.6	34.8	45.5	45.3	45.5	14.1	19.7	38.5	0.0008
0.74	38.4	498.8	40.6	118.6	40.0	48.7	48.4	48.7	15.3	21.4	41.0	0.0008
0.76	41.7	498.7	46.3	118.5	45.6	52.0	51.7	52.0	16.6	23.1	43.5	0.0009
0.78	45.0	498.5	52.7	118.5	51.9	55.4	55.1	55.4	17.9	24.9	46.1	0.0009
0.80	48.5	498.4	59.9	118.4	59.1	59.1	58.7	59.1	19.3	26.9	49.0	0.0010
0.82	52.2	498.3	67.5	118.3	66.6	62.8	62.3	62.8	20.8	28.9	51.7	0.0011
0.84	56.0	498.2	76.4	118.3	75.4	66.8	66.3	66.8	22.3	31.0	54.6	0.0011
0.86	60.1	498.1	85.8	118.2	84.8	70.7	70.2	70.7	23.9	33.2	57.7	0.0012
0.88	64.2	497.9	96.3	118.2	95.3	75.0	74.3	75.0	25.6	35.5	60.8	0.0013
0.90	68.7	497.8	107.2	118.1	106.1	79.1	78.4	79.1	27.4	37.9	63.8	0.0014
0.92	73.3	497.6	119.6	118.0	118.5	83.6	82.8	83.6	29.2	40.4	67.0	0.0014
0.94	78.1	497.5	133.1	117.9	131.8	88.1	87.2	88.1	31.1	43.1	70.3	0.0015
0.96	83.1	497.3	147.6	117.9	146.2	92.8	91.8	92.8	33.1	45.8	73.6	0.0016
0.98	88.4	497.2	163.1	117.8	161.7	97.6	96.5	97.6	35.2	48.6	76.9	0.0017
1.00	93.8	497.0	180.3	117.7	178.8	102.6	101.3	102.6	37.4	51.5	80.4	0.0018
1.02	99.4	496.8	199.0	117.6	197.4	107.8	106.4	107.8	39.6	54.6	84.1	0.0018
1.04	105.3	496.6	218.9	117.5	217.3	113.0	111.5	113.0	42.0	57.7	87.6	0.0019
1.06	111.4	496.4	240.1	117.5	238.4	118.4	116.7	118.4	44.4	61.0	91.2	0.0020
1.08	117.7	496.2	263.1	117.4	261.3	123.9	122.1	123.9	46.9	64.4	94.9	0.0021
1.10	124.2	496.0	288.0	117.3	286.0	129.6	127.6	129.6	49.5	67.9	98.7	0.0022
1.12	130.9	495.8	314.5	117.2	312.5	135.5	133.2	135.5	52.2	71.5	102.6	0.0023
1.14	137.9	495.6	342.9	117.1	340.8	141.5	139.0	141.5	54.9	75.2	106.5	0.0024
1.16	145.1	495.4	373.2	117.0	371.0	147.6	144.9	147.6	57.8	79.1	110.4	0.0025
1.18	152.5	495.1	405.8	116.8	403.4	153.9	150.9	153.9	60.8	83.0	114.4	0.0026
1.20	160.3	494.9	440.2	116.7	437.7	160.3	157.0	160.3	63.9	87.1	118.4	0.0027
1.22	168.2	494.7	477.1	116.6	474.5	166.9	163.3	166.9	67.0	91.3	122.5	0.0029
1.24	176.4	494.4	516.3	116.5	513.6	173.6	169.7	173.6	70.3	95.6	126.7	0.0030
1.26	184.9	494.1	557.9	116.4	555.0	180.4	176.2	180.4	73.7	100.1	130.8	0.0031
1.28	193.6	493.9	602.0	116.2	599.1	187.4	182.9	187.4	77.1	104.7	135.0	0.0032
1.30	202.5	493.6	649.0	116.1	645.9	194.6	189.7	194.6	80.7	109.4	139.3	0.0033
1.32	211.7	493.3	698.9	116.0	695.7	202.0	196.6	202.0	84.3	114.2	143.6	0.0035
1.34	221.2	493.0	751.6	115.8	748.2	209.4	203.6	209.4	88.1	119.1	148.0	0.0036
1.36	230.9	492.7	807.1	115.7	803.6	217.0	210.8	217.0	92.0	124.2	152.3	0.0037
1.38	240.9	492.4	865.9	115.6	862.2	224.8	218.0	224.8	96.0	129.4	156.7	0.0039
1.40	251.2	492.1	926.2	115.4	924.4	232.7	225.4	232.7	100.1	134.8	161.2	0.0040

Description of the columns:

(1) γ , the total angle for which the transformer is in saturation.

(2) GIC , the effective direct current in the transformer.

(3) θ , the angle at which the transformer goes into saturation.

(4) α , the angle at which the transformer goes out of saturation.

(5) I_{R1} , the real component of the exciting current.

(6) I_{x1} , the reactive component of the exciting current.

(7) I_1 , the fundamental component of the exciting current.

(8) I_2/I_1 , the second harmonic in p.u. of fundamental.

(9) I_3/I_1 , the third harmonic in p.u. of fundamental.

(10) I_4/I_1 , the 4th harmonic in p.u. of fundamental.

(11) I_5/I_1 , the 5th harmonic in p.u. of fundamental.

(12) I_{RMS} , the RMS value of the exciting current by direct integration.

(13) I_{RMS5} , the RMS value of the exciting current using upto 5th harmonic.

(14) V_{2RMS} , the RMS value of the secondary voltage (L-L) .

(15) P_c , the increased copper loss due to GIC.

(16) P_I , the iron loss under GIC.

(17) P(IN.), the total increased loss due to GIC.

(18) Q , the total increased Var demand.

(19) Q_2 , the increased Var demand of the magnetizing branch.

(20) S , the apparent power.

(21) S_R , the active apparent power.

(22) S_x , the reactive apparent power.

(23) S_D , the distortion power.

(24) P.F. , the Power Factor.